J. Membrane Biol. 119, 109–132 (1991)
002226319100011T

The Journal of
Membrane Biology

Topical Review

Structure and Function of Channels and Channelogs as Studied by Computational Chemistry

George Eisenman and Osvaldo Alvarez
Department of Physiology and Brain Research Institute, University of California at Los Angeles Medical School, Los Angeles, California 90024-1751, and Department of Biology, Faculty of Sciences, University of Chile, Santiago, Chile

Introduction

Background

Sufficient advances in membrane biophysics, molecular biology, high resolution protein crystallography, and computational chemistry have occurred that it is beginning to be possible to calculate the energetics of ion interactions with any protein structure known at high resolution. In the case of ion channels, which are proteins that span biological membranes and provide a pathway for ions, it is now feasible to calculate the free energy along the ion path. Since the free energies along the reaction path underlie the electrical properties of the channel, such calculations enable function to be predicted from structure. Conversely, important details of a channel's structure can be deduced from a knowledge of its electrical properties. This paper shows examples of such calculations and discusses how they can be performed. It emphasizes what can be learned by studying several channel-like analogues in icosahedral viruses (which we will call "channelogs") whose coordinates are known crystallographically at atomic resolution. It also makes calculations for certain less reliably known, but fairly well-agreed upon, structures postulated to exist for several functionally well-characterized channels. The family of viral channelogs encompasses structures with a common pentameric architecture [79, 80] and with narrow regions analogous to selectivity filters [47] which can be lined by negative or positive dipoles [52] or even positively charged residues [84]. The channelogs also contain wider regions with a variety of geometries and polar linings which can provide models for channel "vestibules" [11–13, 100]. They therefore provide interesting models for cation and anion channels and their cation and anion binding sites.

Key Words channels · energy profiles · molecular dynamics · molecular mechanics · structure · function · icosahedral viruses · acetylcholine receptor channel · gramicidin · ion permeation · ion selectivity

Outline of What Will be Presented

After an initial description of several structures whose expected permeation properties will be calculated, the paper shows how the energy profile can be computed for a variety of three-dimensional channel structures, both known and speculative. We start with the simplest, crystallographically known, channel-like structure occurring between protein subunits, which is found on the fivefold axis of the protein capsid of icosahedral viruses such as the satellite tobacco necrosis virus (2STV), the human *rhinovirus* (2RHV), the southern bean mozaic virus (4SBV), the tomato bushy stunt virus [45, 72] as well as the Polio virus, the Mengo virus [64*a*] and many others [80] (we abbreviate the ones referred to in the text using the nomenclature of the Brookhaven Protein Data Bank [6]). Architecturally, these structures can be simply hourglass shaped [52], with a narrow region in the middle, which can function as a "selectivity filter" [47] where ion discrimination occurs and relatively wide entrances. They may also contain a series of widenings and narrowings, where the wider regions can function as "vestibules" [11, 14, 55, 100] in which interactions with ionizable, dipolar, and hydrophobic groups can modify the concentrations of permeant species from those in the bulk solution. We will call such structures *channelogs* because of their structural analogy to membrane channels. In the simplest of these channelogs, found in 2STV [52], the selectivity filter consists of

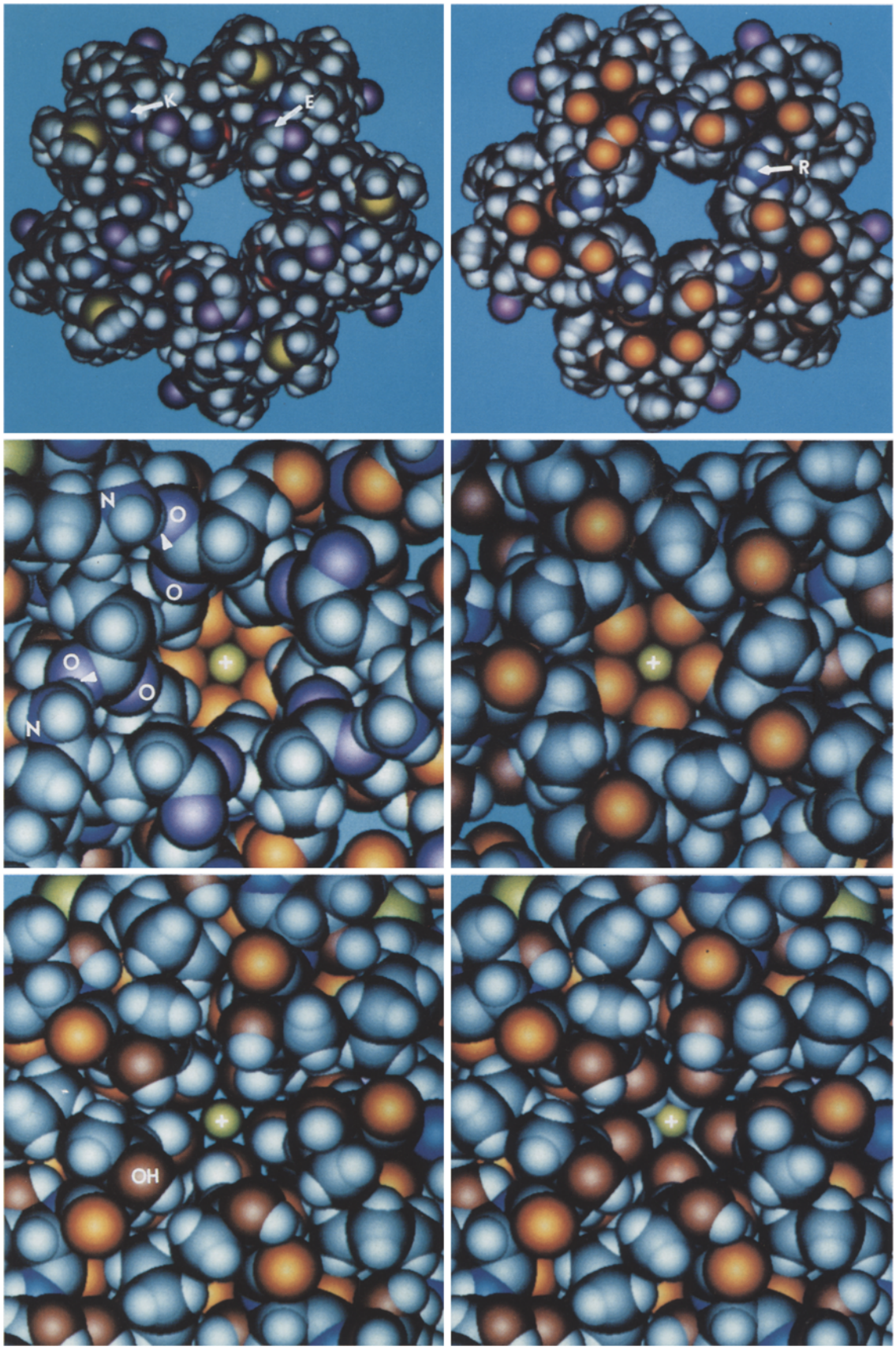
K
E
R
N
O
O
O
O
N
+
+
+
OH
+

a narrow ring of five backbone carbonyl oxygens surrounding a 2-Å diameter aperture (*see* middle pair of color plates in Fig. 1). In other channelogs the filter can be chemically the same but wider (4 Å in 2RHV [27, 78]) or can be composed of different ligands, such as side-chain threonine –OH's in 4SBV [21, 77] (*see* bottom pair of color plates in Fig. 1) or even arginine –NH's in Cowpea Mozaic Virus [84]. We first present calculations for the energy profile for the fivefold channelog in 2STV, the smallest and simplest icosahedral virus, and then for 4SBV in which the selectivity filter in the fivefold channelog is formed not from backbone carbonyl oxygens but by side-chain hydroxyl groups.

We next examine a proposed structure for a topologically similar channel, the M2delta pentamer proposed [17] for the channel lining of the acetylcholine receptor (AChR) channel (*see* top pair of color plates in Fig. 1). This conjectured structure is examined, not because it is necessarily correct in all details, but to illustrate an important difference in the permeation properties of channels formed from pentamers of beta barrels as in the viruses *vs.* pentamers of parallel alpha helices as in all proposed structures for membrane channels [cf. 4, 9, 42–44, 58]. The calculations up to this point are restricted to computations with a laboratory microcomputer for structures whose atoms are "frozen" at their initial (crystallographic) positions, using a Langevin dipole approximation to represent water molecules [27, 96].

Such simplified calculations can provide a number of insights into permeation, particularly as to the energetic factors controlling which species permeate and how well, what the effects of simple point mutations might be, and what effects helix dipoles and ionizable residues might have. However, they cannot assess energy profiles as reliably as calculations in which water molecules are treated explicitly and where the protein atoms are allowed to rearrange as ions are moved through the structure. Such calculations require a molecular dynamics simulation, which can no longer be done on a microcomputer but can be carried out on a laboratory minisupercomputer. We summarize how this calculation has been done for gramicidin by Aqvist and Warshel [3] and then apply molecular dynamics and free energy perturbation procedures to re-examine the energy profile for ion permeation in the 2STV channelog to determine if such a structure could permit ion transport at a sufficiently rapid rate to function as a channel.

The paper concludes with a brief description of ion selectivity for several frozen selectivity filters and an attempt at relating the findings for these to earlier selectivity modelling using rearrangeable nearest neighbor interactions [15–20] and of "sieving" type steric filters [68, 69]. Somewhat surprisingly, the computed selectivity for all the frozen filters examined to date is found to fall into the same pattern of so-called "Eisenman sequences" as in previous "field strength" modelling of binding sites with rearrangeable structure. Narrow filters (or binding sites) show a formal equivalence to those having high field strength in that they produce typical "high field strength" selectivity sequences [15, 16], whereas wide filters show a formal equivalence to those having low field strength. The computations do take into account interactions with distant atoms in the protein (which earlier modelling [15–18] did not); but for frozen coordinates, such interactions are the same for all ions of the same charge, and are therefore species independent for all like-charged

Fig. 1 (COLOR PLATE). This figure was drawn with a PGA graphics card using Robinson's and Crofts' Protein Data Viewer (PDV) program [76]. Atoms are represented by spheres with the following CPK radii: oxygen, 1.5 Å; nitrogen, 1.55 Å; carbon, 1.7 Å; hydrogen, 1.1 Å; sulfur, 1.8 Å; the scale can be judged from the radius of oxygen which is 1.5 Å. Different kinds of protein oxygens are distinguishable by their color coding: backbone carbonyl oxygens are orange, side-chain hydroxyls are red, and side-chain carboxyls or carbonyls are purple. Nitrogens are colored dark blue, carbons blue-grey, sulfurs yellow, H atoms white. No water molecules are shown. *Top:* Space-filling model proposed for the ion channel region formed between the M2delta subunits of the AChR channel. The left and right views are from the inside (cytoplasmic) and outside (synaptic) surfaces of a space-filling representation down the fivefold axis of Oiki et al.'s proposed structure of the M2delta pentamer of the acetylcholine receptor channel [71]. The heavy atom coordinates have been supplied by Vincent Madison, and H atoms have been added with Warshel's PDLD program [96]. This figure shows how five alpha helices come together on the fivefold axis to form a pentameric structure surrounding a channel. Notice that the narrowest portion of the channel (at 10 Å) is formed by a ring of side chains from five threonines (THR_5). This corresponds to the ion binding site nearest the cytoplasm found in the calculations. In this proposed structure the methyl groups are actually slightly closer to the channel axis and hide the deeper hydroxyl groups in this view. A further narrowing of the channel is seen at 20 Å, which is lined by five phenyl side chains from PHE_{16}. This corresponds to another ion binding site found in the calculations. *Middle:* Space-filling representation of the pentameric channel-like structure found on the fivefold axis of the satellite tobacco necrosis virus [52]. The left view is from the inside looking out, the right view is from outside looking in. The pentamer was made using the PDV program by successive 72° rotations of the monomer around the fivefold axis, and hydrogens were added by the PREPARE subroutine of POLARIS [93] and have not been energy-optimized. Further description is in the text. *Bottom:* Space-filling representation of the pentameric channel-like structure found on the fivefold axis of the Southern Bean Mozaic Virus [83]. Both views are from outside looking in. The left view shows the H's of the selectivity filter rotated maximally away from the channel axis (upard toward the viewer). The right view shows the H's rotated maximally toward the channel axis. This is further described in the text

ions. Species-dependent selectivity among the alkali metal cations or the halide anions in a rigid system with frozen protein coordinates is therefore determined solely by local (van der Waal's repulsive) interactions. By contrast, in systems whose structures are permitted to rearrange, the energy of rearrangement, as well as energy contributions from more distant atoms are involved, which has implications for whether replacements are isomorphous or nonisomorphous, as well as for whether or not allosteric interactions occur.

Structures

Two kinds of protein channels are known to exist: one is formed as a pore *within* a protein, the other as a pore *between* protein subunits. Gramicidin [59, 87, 91] typifies the former in which a cylindrical channel occurs within the lumen of a beta helical structure that utilizes the carbonyl oxygens of the peptide backbone to form a polar interior. Examples of the latter type are shown in Fig. 1 (Color Plates). At the top is a space-filling model of the ion pore region in a speculative structure proposed for the acetylcholine receptor (AChR) channel [17], which occurs *between* transmembrane bundles of alpha-helices and is typical of all known intrinsic membrane channels [4, 7, 9, 33, 36, 37, 41, 42–44, 49–51, 70, 71, 101]. There is a clear similarity to this pentameric structure in the crystallographically known channel-like structures found on the fivefold axis of icosahedral viruses shown in the middle (2STV) and bottom (4SBV) color plates (Fig. 1).

In all these figures, drawn using Robinson's and Crofts' Protein Data Viewer (PDV) program [76], atoms are represented by spheres with the following CPK radii: oxygen, 1.5 Å; nitrogen, 1.55 Å; carbon, 1.7 Å; hydrogen, 1.1 Å; sulfur, 1.8 Å; and the scale can be judged from the radius of oxygen which is 1.5 Å. Different kinds of protein oxygens are distinguishable by their color coding: backbone carbonyl oxygens are orange, side-chain hydroxyls are red, and side-chain carboxyls or carbonyls are purple. Nitrogens are colored dark blue, carbons blue-grey, sulfurs yellow, H atoms white. No water molecules are shown.

A Speculative Structure for the Acetylcholine Receptor Channel

The left and right color plates at the top of Fig. 1 show views from the inside (cytoplasmic) and outside (synaptic) surfaces of a space-filling representation down the fivefold axis of Oiki et al.'s proposed structure of the M2delta pentamer of the acetylcholine receptor channel [71]. The heavy atom coordinates have been supplied by Vincent Madison, and H atoms have been added by the PREPARE subroutine of the POLARIS program [96]. This figure shows how five alpha helices come together on the fivefold axis to form a pentameric structure surrounding a rather wide channel. The fivefold symmetry is apparent, as is the closeness of packing between the pentameric subunits.

The sequence of the 23 residues of the M2delta segment is, from internal to external:

GLU_1–LYS_2–MET_3–SER_4–THR_5–ALA_6–ILE_7–
SER_8–VAL_9–LEU_{10}–LEU_{11}–ALA_{12}–GLN_{13}–
ALA_{14}–VAL_{15}–PHE_{16}–
LEU_{17}–LEU_{18}–LEU_{19}–THR_{20}–SER_{21}–GLN_{22}–
ARG_{23}

Noteworthy are the presence of rings of ionizable residues GLU_1 (labeled "E") and LYS_2 (labeled "K") at the inner end of the channel and ARG_{23} (labeled *R*) at the outer end. In the view of the inner face (left) the GLU residues can be seen to form a rather wide ring of 10 carboxylic oxygens (purple) while the LYS residues make a ring of five $-NH_3$'s somewhat more distant from the axis. (The –NH groups visible nearest the channel axis are the amino terminals of GLU_1, which in the full channel structure connect to the next residue). In the view of the outer face (right) the guanidino groups of each arginine are visible. Also visible on the outer surface are the C-terminal carbonyl oxygens (orange) that in the full channel structure would bind to the next residue. The narrowest portion of the channel is formed by a ring of side chains from five threonines (THR_5).

This channel is wide and its lumen is reasonably polar, so one might expect it to be easily permeable to ions. One of the important reasons for bothering to compute the energy profile implied by this structure is to check this expectation. Indeed, we will find that the solely visual perception is misleading because it leaves out what is not visible, namely the electrostatic effects of the five parallel alpha helices in this structure. The PDLD calculations presented below show that the parallel alpha helices produce such a large electrostatic potential on the channel's axis that, if uncompensated, this sterically open channel would be completely impermeable to ions! The calculations will also show how H^+ ionization from the rings of ionizable –COOH and $-NH_2$ residues bounding the two ends of the proposed channel structure can compensate this electrostatic potential in a self-regulatory (homeostatic) way.

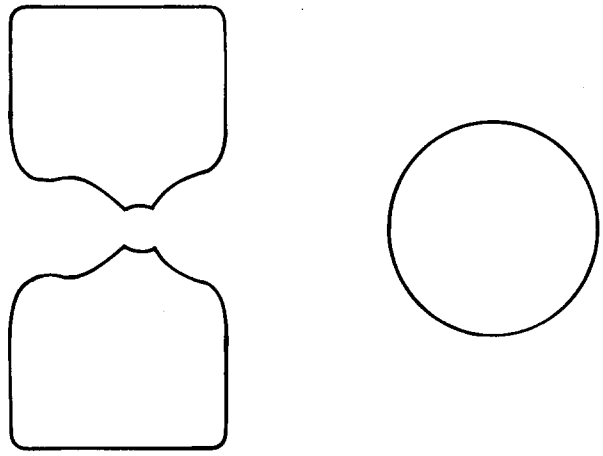

Fig. 2. Diagram of procedure for calculating energy profile for ion permeation. A section along the fivefold axis of the 2STV viral channelog is shown at the left. At the right is shown a sphere of 12 Å radius which is moved as a "probe" along the fivefold axis and within which all interactions are calculated microscopically as described in the Appendix

The Crystallographically Known Structure for the Channelog in 2STV Exemplifying a Carbonyl Selectivity Filter

In contrast to the conjectured structure for the AChR channel, the structure for the channelog found on the fivefold axis of 2STV shown in the middle of Fig. 2 is known at atomic resolution from X-ray crystallography studies by Jones and Liljas [52]. This structure is hour-glass shaped with its narrowest region being an aperture of 2 Å diameter formed by a ring of five backbone carbonyl oxygens (orange). A view from inside is shown at the left, from outside at the right. Although it is hard to see the architecture of these channelogs in a nonstereoscopic view, the reader should imagine when looking at the views of 2STV in Fig. 1 that he is viewing the narrow ring of five carbonyl oxygens of the selectivity filter through a rather narrow funnel-shaped vestibule from the inside (left) and through a shallower funnel-shaped vestibule from the outside (right). The fivefold symmetry is apparent as is the closeness of packing. An ion is observed to be bound in the plane of this ring [52] and is shown as 2-Å diameter yellow sphere (labeled "+"). This ion is present in the crystallographic data and is almost certainly Ca because of its electron density and ligand distances. The coordination of the Ca ion is completed on the fivefold axis by one water molecule above and one water molecule below the plane of the ring. These water molecules have been removed in Fig. 1 so the ion can be seen. The ring of oxygens corresponds physically to what is commonly regarded as a selectivity filter [47], as will be borne out by the calculations to be presented below.

The aperture is formed by a ring of five backbone carbonyls contributed by THR_{138} from each of the pentamerically related monomers. This site is an example of the ability of proteins to bind cations solely by interactions with the peptide backbone, as in peptides like valinomycin and gramicidin [23]. Indeed, this site is a clear example, and the only presently known one, of such a purely *backbone* binding site in a protein (*sic*). This kind of architecture is encountered in all the known icosahedral viruses, and a pentameric ring of backbone carbonyl oxygens is also found in the analogous structure in the human *Rhinovirus* [79, also *see* 27], although the hole in the ring is twice as wide as in 2STV (being 4 Å rather than 2 Å in internal diameter). Similar carbonyl rings are found in the Mengo and Polio Viruses [80].

An important detail visible in the internal view is a ring of 10 side-chain carboxylate oxygens (purple) from GLU_{140} lining the channelog some 5.5 Å internal to the selectivity filter [52]. The –COO oxygens of two of these have been labeled *O*. This relatively wide ring is the analogue of the kinds of dissociable groups postulated to exist in the vestibules of various membrane channels [11, 100]. The effects of dissociation of H^+ from this ring to alter the energy profile, and thus modulate ion conductance, are examined in a later section. Also visible is the ring of five Lys_{141}–NH_2's, two of whose nitrogens have been labeled *N*. One can see that the five Lys_{141}–NH_2 H's are positioned so that they could form H-bonds with the Glu_{140} carbonyl oxygens, as indeed they do in an optimized structure (the H's in Fig. 1 are not in their optimized positions but two H-bonds are indicated by arrows).

The structure "looks" like a channel, as was recognized by Jones and Liljas [52]. Whether or not it could actually function as a channel is examined in a later section; but it is clear from the X-ray data alone that the ring of backbone carbonyl oxygens can provide a binding site for Ca (and presumably other cations) and that such ligands can replace a major portion of the primary hydration shell. In addition, ion depletion studies [67] indicate that this site is highly selective for Ca, with dissociation constants in the micromolar or submicromolar range. The results of the energetic calculations described below are compatible with these observations.

The antiparallel loop structure of the beta barrel pentameric subunits provides no strong electrostatic

fields like those of the parallel alpha helices to interfere with ionic permeation. However, modulation of the energy profile by ionization of H^+ from the ionizable Glu_{140} and Lys_{141} rings can alter permeation and binding substantially, and an example of how such effects can be assessed will be shown.

The Crystallographically Known Structure for the Channelog in 4SBV Exemplifying a Hydroxyl Selectivity Filter

The kind of selectivity filter formed by *side-chain* hydroxyl groups is illustrated at the bottom of Fig. 1 based upon the crystallographic data for 4SBV [82, 83]. The left and right views are both from the external perspective but differ in that they show the positions of the H atoms in the selectivity filter when these have been rotated maximally away from the channel axis (left) and maximally towards it (right). The selectivity of these two limiting configurations will be described below. Note that the arrangement of the –OH groups in the selectivity filter is formed by THR side chains that are exposed by a beta turn at the narrow end of the wedge-shaped beta barrels.

An ion (colored yellow) having a diameter of 2 Å, whose existence is purely hypothetical, has been added to the data at the locus calculated energetically for the binding site so that the selectivity filter can be seen more easily. The site is "ambidextrous" [29]. At the left the ion can be seen to be in contact with five hydroxyl *oxygens* when the H's (colored light blue) have been rotated to face maximally away from the axis of the channel (i.e., toward the viewer). When the hydroxyl H's have been rotated maximally toward the channel axis (right-hand plate), the ion is seen to make close contact with five hydroxyl *hydrogens*. When the –OH's face inward, the calculations will show that a binding site for an anion is expected because of favorable coulombic interactions with the positive hydrogen ends of the –OH dipoles. On the other hand, the calculations will show that when the –OH dipoles face away, a binding site for cations could also exist.

In the view of the external face of 4SBV the reader should also note the rather wide ring of five Thr –OH's at the superficial surface of the funnel-shaped vestibule leading to the selectivity filter. One of these is labeled *OH*. These are a physical embodiment of the dipolar type of group that has been suggested might be present in a channel vestibule [11]. From an internal view (*not shown here*) one would be looking down a rather long bulbous tube with a central bulge internal to the selectivity filter. Indeed, the differences in architectural detail between the various viral fivefold channelogs provide a nice set of channel structures and linings for comparative studies for which PDLD calculations are particularly appropriate [27, 29].

Energy Calculations for Known or Conjectured Structures

Attempts to evaluate the energetics of interactions in proteins from a knowledge of their structure date back to the macroscopic approaches of Linderstrom-Lang [64] and of Tanford and Kirkwood [86]. From these beginnings computational chemists have developed a number of powerful molecular dynamics or molecular mechanics energy minimization algorithms which can be implemented on laboratory micro and minicomputers. Available programs are AMBER [5, 98], CHARMM [10], DELPHI [40], GROMOS [88, 89], MM2 [10a], DREIDING [66], POLARIS [96], or MOLARIS [93].

These procedures represent the total energy by means of a *force field* which approximates the exact wave equation description as a superposition of simplified analytical expressions for various two-body, three-body, and four-body interactions. This permits rapid evaluation of the forces on all particles, from which the optimum geometry and dynamics of motion are evaluated. The former procedure is referred to as molecular mechanics, the latter as molecular dynamics [*cf.* 66]. These approaches differ chiefly in their choices of force fields and the way in which H-bonded interactions are represented. The potential energy of the system is generally expressed as a sum of bonded, nonbonded, and constraint energies. Typical bonded interactions are bond stretching, bond angle bending, dihedral angle torsion, and inversion. Nonbonded interactions are van der Waal's, electrostatic, induced dipole, and H-bonding (when not treated electrostatically). Because the number of nonbond interactions increases as the square of the number of atoms, long-range cutoff distances are usually invoked to reduce the computational requirements.

Three Levels of Approach

Three levels of calculation will be described, each with its own particlar advantages, drawbacks, and appropriateness to a particular problem. The simplest level is the use of Warshel's Protein-dipole Langevin-dipole (PDLD) algorithm on known or conjectured three-dimensional structures whose

atoms remain fixed or "frozen" during the computation. This procedure presents a simple way of modelling hydration by assigning a grid of Langevin dipoles to all interstices into which water molecules might fit. It is computationally nonintensive and can be easily carried out on a 32-bit microprocessor such as the Definicon DSI 780 that we used or the Intel 80386/80387. It is particularly appropriate for exploring the general ion permeation (or binding) properties of any conjectured structure and will be shown, by analyzing a proposed model of the acetylcholine receptor channel, to be useful for revealing important effects of such nonvisually obvious long-range force fields as those resulting from helix dipoles of parallel alpha helices. Its usefulness for examining the effects of "computer mutations" on permeation energy profiles is also demonstrated.

The next level of modelling, the energy minimization/protein-dipoles Langevin-dipoles [96] (EM/PDLD) approach, involves first allowing the protein to minimize its structural energy by molecular dynamics simulations and then applying PDLD calculations to the energy-minimized structure. In such calculations, a number of explicit water molecules can be represented and the energy profile can be determined along the optimum free energy path. This kind of computation requires a minicomputer and will be exemplified by Aqvist and Warshel's studies of the gramidicin channel [3]. It is particularly appropriate for structures which are reasonably well known.

The most computer-intensive level of modelling to be described here, but one still capable of being performed on a laboratory minisupercomputer, is the molecular dynamics and free energy perturbation (MD/FEP) procedure which will be exemplified here by the calculation of the free energy profile for Na passing through the fivefold selectivity filter of 2STV. This level of modelling is only justifiable for a crystallographically known structure and is appropriate for obtaining detailed information about the structural and energetic changes that occur for example when replacing an ion by another of differing size and/or charge, or when trying to determine the minimum energy profile for moving an ion through a well-defined channel structure.

I. PDLD Calculations

Computation

The present PDLD computations for "frozen coordinates" were performed on a laboratory microcomputer using POLARIS, Warshel's protein-dipoles Langevin-dipoles (PDLD) program [96] modified by F. Bezanilla to run on a 32-bit coprocessor board (Definicon DSI/780+).

Energy Profiles

The procedure for computing the energy profile is conceptually quite simple. Figure 2 illustrates how this is done. A probing sphere of 12 Å radius, immersed in a medium of dielectric constant 80, containing an ion of given size and charge at its center and filled with a grid of Langevin dipoles, is moved along the fivefold axis from a position far to the right, through the protein, to a position far to the left, and the total energy of the system is computed at each point. The total energy at any position is the sum of the following individual terms: Q, the ion-charge energy; D, the ion-induced dipole energy; V, the Van der Waal's energy; and L, the Langevin dipole energy. Each of these energies is computed microscopically by the PDLD program for all atoms within this sphere as the difference between the energies of the system when the ion is uncharged and charged. The total energy also includes a macroscopic Born energy (B) external to the sphere (*see* [96] and the Appendix for details).

When the probing sphere is far enough from the protein that ion-protein interactions are negligible, the energy is due solely to the Langevin and Born terms and should correspond to the energy of hydration. On the other hand, when the ion is located at the selectivity filter, the total energy should correspond to the energy of binding. In between these extremes the total energy represents the energy of the system for a given position of the ion. Therefore, a plot of the total energy *vs.* distance should yield a quantitative picture of the free energy profile for permeation. The results are illustrated in Fig. 3.

It will be shown below that the energy profile arises as a balance between ion-water and ion-protein interactions. As an ion proceeds from the solution into the channel, hydration energy is lost as it enters the narrower regions of the channel and fewer and fewer water molecules become available to hydrate it. However, this loss of hydration energy is made up by the energy that is gained from increasing interactions with the protein as the selectivity filter is approached, until finally the binding energy reaches its maximum at the mid-point of the annulus comprising the selectivity filter, where the total energy can be seen to have its most negative value.

To forestall confusion, the reader is reminded that, though absolute values of free energy will be presented throughout this paper, it is only the differ-

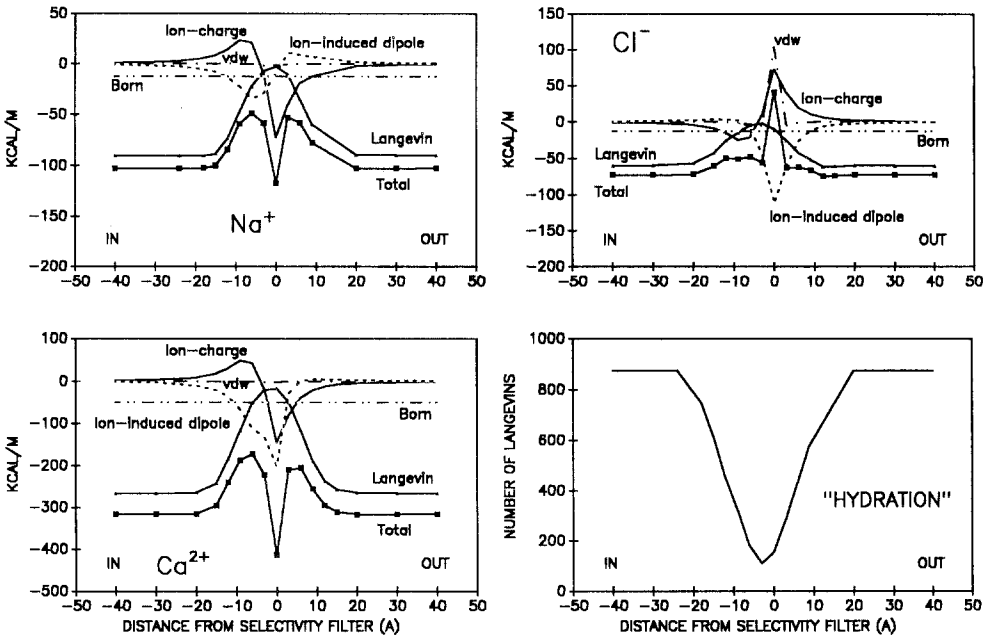

Fig. 3. Energy profiles and extent of hydration as a function of distance from the selectivity filter for the Satellite Tobacco Necrosis Virus. Distances in Å

ence in energy of the ion at any point in the channel, relative to the reference state of the ion *in water* far from the channel, that is relevant to ion permeation. The energy profile for permeation is therefore given by the changes in energy level of the "total" curve in relation to the asymptotic value of free energy which is seen at a great distance from the channel.

Free Energy Profile for a Viral Channelog whose Selectivity Filter is Formed by Backbone Carbonyl Oxygens

The computation of the free energy profile for ion permeation will begin with a calculation for the structurally simplest pentameric viral "channel," that of 2STV shown in the middle section of Fig. 1. The first questions to be asked for this putative channel are: is it expected to bind cations, as observed experimentally [52, 67], and is it more permeable to cations than anions, as expected intuitively for a carbonyl oxygen selectivity filter?

The free energy profiles computed for Na^+, Ci^- and Ca^{2+} permeation are presented in Fig. 3. The energy profile for Na^+, given by the curve labeled "Total," is seen to consist of an energy minimum (i.e., a binding site) at the selectivity filter separated from the fully hydrated reference levels by two relatively symmetrical energy maxima (i.e., barriers) to entering and leaving the site from or to the adjoining solutions. In channel parlance [47, 60], this corresponds to the two-barrier one-site profile. In the case of Cl^- a sharp maximum exists at the selectivity filter, corresponding to a strong repulsion. The "channel" therefore is expected to bind Na^+ but not Cl^- and also to be much more permeable to Na^+ than to Cl^-. The channel prefers Na^+ over Cl^-, not only because the electrostatic interaction is unfavorable but also because the van der Waals repulsion energy for Cl^- is large.

Note that the hour-glass shape of the channel correlates nicely with the number of water molecules found in it. This can be seen in the lower right part of Fig. 3, which plots the number of Langevin dipoles contained in the probing sphere as a function of distance from the selectivity filter. This number is a measure of the number of water molecules in the channel. Notice how water is increasingly excluded as one gets nearer to the selectivity filter region.

The profile for Ca^{2+} resembles that for Na^+ except that the minimum for the total energy is deeper for Ca^{2+} than for Na^+. This implies that Ca^{2+} is more strongly bound than Na^+ to this channel, in accord with experimental findings [52, 67]. The relative preference for divalent over monovalent cations is, of course, a function of the value of the partial charge on the carbonyl oxygen and carbon (the value usually assumed is 0.383, which was parametrized for zero polarizability [95]; 0.15 was used for Fig. 3 to compensate for the inclusion of a substantial polarizability component of the carbonyl oxygens). The effects of partial charge on selectivity have been discussed elsewhere [27, 29]. For larger values of

partial charge the divalents will be even more preferred, and vice versa.

The general features of the profile are consistent with current views as to what is expected for a cation channel. The magnitudes of the energies calculated using the simple Langevin-dipole representation of water are much more reasonable than the many hundreds of kcal/M calculated in an earlier model of the 4SBV channelog [82] which did not include water. However, the profile is not satisfactory quantitatively, for it implies impossibly slow ion exchange for a ring of carbonyl oxygens. For example, the barrier for Na to leave the ring to the outside is about 60 kcal/M and to enter is about 50 kcal/M. Since a barrier of 50 kcal/M implies a rate of motion slower than 1 ion per 10^{16} years, permeation through a structure with such an energy profile would be too slow for it to function as a channel. Indeed, such a channelog would not even be able to exchange an ion on the time scale of ion displacement studies [67]. The unrealistically strong binding and impossibly slow permeation rates implied by the present energy profile are due to inadequacies, discussed below, of the Langevin-dipole procedure for modelling water in narrow regions. This result indicates that simple PDLD modelling may not be appropriate for quantitative assessment of such an energy profile, and, indeed, we will reassess this energy profile by the more rigorous MD/FEP procedure in a later section.

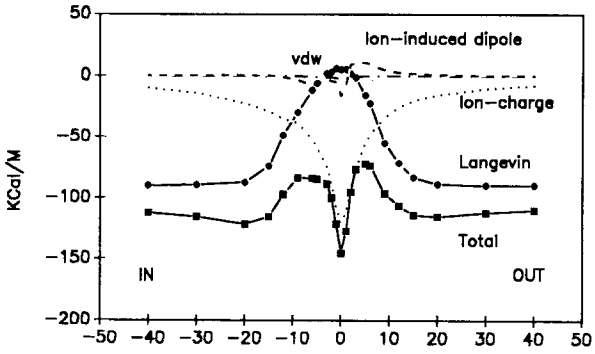

Fig. 4. Effect of ionizing the ring of Glu_{140} on the energy profile for Na permeation in the fivefold channelog of the Satellite Tobacco Necrosis Virus. This was plotted in the same manner as Fig. 3, but with an excess negative charge of -1 distributed uniformly over the carboxylate oxygens of all five Glu_{140} residues

Effect of Ionizing a Neighboring Ring of Carboxylate Oxygens

The viral channelog provides a system in which one can explore the effects of charged vestibules. For example, we examine here the effect of ionizing the ring of side-chain carboxylate oxygens from GLU_{140} previously noted to be located some 5.5 Å internal to the selectivity filter. For the calculations in Fig. 3 this ring was assumed to be uncharged (i.e., the dissociable H^+ is assumed still to be bound). The interactions of an ion on the channel axis with this ring can be seen in the ion-charge and ion-induced dipole energies at -5.5 Å from the selectivity filter (the interactions produce the second dip in the ion-induced dipole energy seen for Na^+ and Ca^{2+}). The ion-charge and ion-induced dipole effects roughly cancel each other, with the ion-charge term being weakly repulsive and the ion-induced dipole term being weakly attractive. However, if dissociation of a single proton from this ring of carboxyls is assumed to occur, this can be modelled by distributing a net negative charge of -1 over all the carboxylate oxygens. Figure 4 shows the profile for Na^+ in this case. It can be seen that the ion-charge energy, which was previously calculated to be repulsive in Fig. 3 in the inner portion of the channelog, becomes strongly attractive in Fig. 4 (*compare* the energies between $x = -5$ and -30 Å in Figs. 3 *vs.* 4). Indeed, the affinity of the site for Na^+ can be seen to be increased by about 20 kcal/M. In addition, the heights of both barriers relative to the aqueous solution are reduced by more than 10 kcal/M; and the permeability of the channel, which is inversely related to the height of the largest barrier relative to the aqueous solution [47], is correspondingly increased. The rate determining barrier has also changed since the internal barrier which was the higher one in Fig. 3 is now the lower one.

Discussion and Conclusions Drawn from the Frozen Structure Analysis

The permeation properties of this viral structure are defined by the energy profiles shown in Figs. 3 and 4. The peaks determine the kinetics and the wells determine the equilibrium properties of ion transport. The present level of modelling is less reliable for the peaks than for the wells. This is because the structure when the ion is in the site is an optimized, equilibrium structure (for Ca). On the other hand, the implications in Figs. 3 and 4 for the activation energies for entering and leaving the ring of carbonyl oxygens, which are of course what determine permeability [25, 47, 60], are considerably less reliable for three reasons. First, the minimum energy path may not lie exactly along the channel axis (for example, the ion might prefer to move along the wall). Second, the atomic structure may rearrange significantly for each position of the ion's trajectory in passing through the channelog, which will have energetic consequences which cannot be examined with the PDLD method. Third, and most important, the

shape (and size) of the barrier is exquisitely sensitive to the point-by-point differences between the energies of hydration *vs.* the energies of interaction with the protein, and the Langevin approximation for the energies of interaction with water molecules doesn't calculate this shape accurately enough. The Langevin procedure is only a first approximation, which is particularly inadequate in narrow regions. Even if the spatial dependence of the energies of interaction with the protein were accurately known, the evaluation of the spatial dependence of the energy of dehydration is too crude to predict permeation quantitatively. These limitations can be removed by including explicit water molecules in an MD/FEP computation as shown in a later section.

Free Energy Profile for a Viral Channelog with a Selectivity Filter Lined by Side-Chain Hydroxyl Groups

The pentameric viral channelog in 4SBV offers a model system in which to explore a selectivity filter formed by –OH groups (recall Fig. 1, bottom). Channels with –OH ligands in their selectivity filters are more complicated than those with backbone carbonyl ligands because the –OH groups can have different orientations of their dipoles relative to the channel axis. Such ligands are of considerable interest because side-chain –OH groups (e.g. from Ser, Thr, or Tyr) are prime candidates for the polar lining of cell membrane channels, and synthetic serine-rich membrane-spanning alpha helices, designed to form polar pores lined by –OH residues, have, indeed, been found to produce cation-selective channels [61, 71]. That these synthetic structures are cation selective seems paradoxical since side-chain –OH's in polyene antibiotic channels are usually ligands for anions rather than cations [31, 34], owing to their ability to orient themselves with the H end of the –OH dipole facing the ion. However, Perutz [73] has pointed out that the gamma–OH of serine in an alpha helix donates a hydrogen bond to the carbonyl oxygen of the next helical turn, so that its lone-pair electrons point away from the helix and has suggested that a ring of serines might in this way form a cation-binding structure.

The computations presented here show how different orientations of the hydroxyl group might enable a selectivity filter to be cation selective in certain situations while being anion selective in others. In particular, they are intended to shed light on how a superfamily of architecturally and chemically similar transmitter-gated channels lined by hydroxyl groups [4] can contain members some of which can be selective for anions [8] while others are selective for cations [1, 14], a finding which till now been rationalized by invoking the conditioning effects of charged groups in the vestibules [8, 11].

The "frozen" level of modelling will now be partially relaxed for the selectivity filter by allowing the side-chain threonine hydroxyl ligands in the selectivity filter of the 4SBV virus (*cf.* the bottom of Fig. 1) to rotate freely around their –C–OH single bond in order to explore the effects on ionic selectivity of allowing hydroxyl ligands to orient with the positive end of their dipoles facing the middle of the channel or away from it. Figure 5 shows the energy profiles for K and Cl calculated for 4SBV in the same way as in Fig. 3, but for the two different orientations of side-chain hydroxyl ligands shown in Fig. 1. The profiles are computed for two extreme conditions: one, when the H ends of the –OH dipoles are rotated so that they face maximally *in* toward the lumen of the channel; the other, when they are rotated so as to face maximally *away* from the lumen. The partial charge of the –OH dipole has been parameterized to include a polarizability component [95]). Accordingly, a charge of $+0.1$ has been assigned to the H atom and of -0.1 to the O atom. Similar profiles are seen for larger and smaller values of partial charge, as well as for different polarizabilities. The effects of varying partial charge on cation- *vs.* anion-selectivity has been examined elsewhere [29, 36].

Cation Permeation Typified by K

The energy profiles computed for K are shown at the top of Fig. 5 for these two cases: when the Thr –OH's rotated *in* (top left) and *away* (top right). The alert reader will notice that the internal barrier is indeed so high in this PDLD calculation that it would preclude permeation. Again, this is because of the exclusion of water in the narrow region of the channelog internal to the selectivity filter and the underestimation of hydration energies in narrow regions by the PDLD procedure [30]. The present discussion will therefore be restricted to entry and exit from the outside of the channelog. Whether this barrier is actually expected to be this large in a more definitive EM/PDLD or MD/FEP calculation remains to be explored.

When the Thr –OH's face *in* toward the lumen (Fig. 5, top left), the energy profile for K is seen to consist solely of an unfavorable energy barrier separating the solutions on the two sides. Such a profile implies that the channel, when its selectivity filter is in this conformation, is impermeant to K. In contrast, when the Thr –OH's face *away* from the lumen (Fig. 5, top right), the energy profile exhibits a distinct energy minimum. Such a profile corresponds to a favorable binding site for K separated by barriers from the internal and external solutions, the

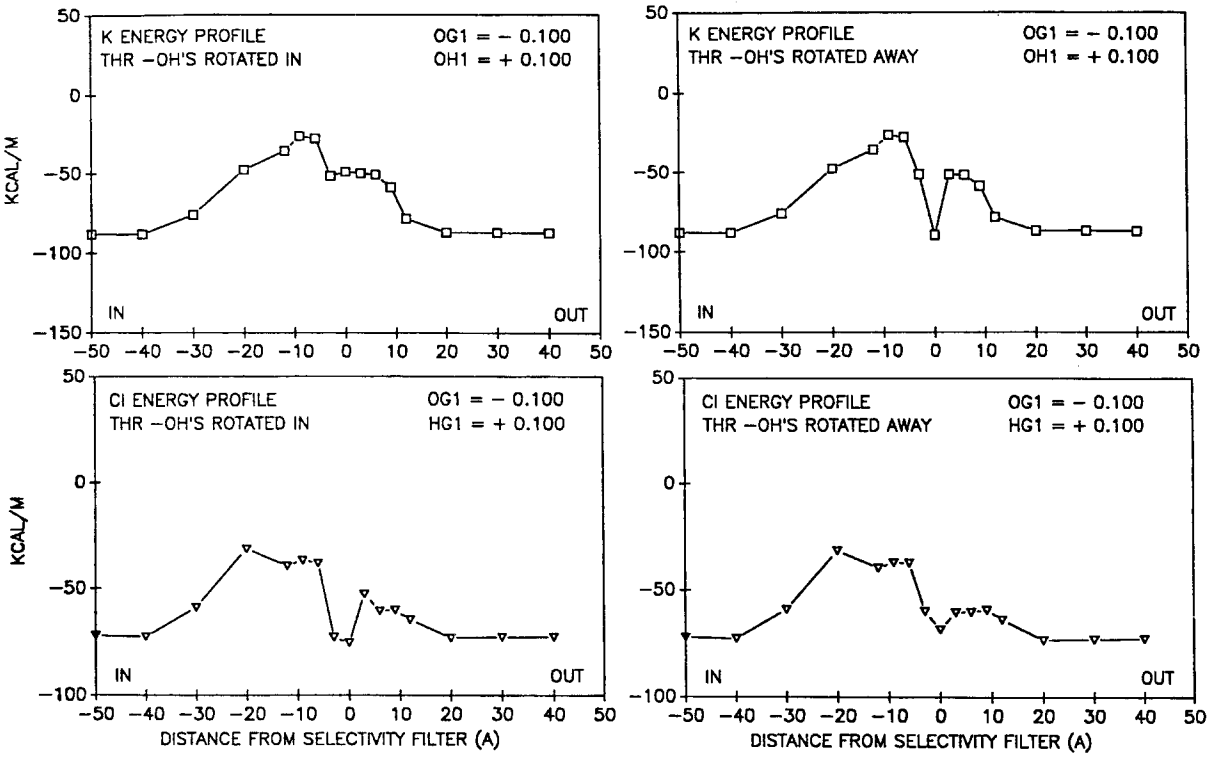

Fig. 5. Energy profiles calculated for a selectivity filter composed of side-chain hydroxyl ligands. The plotted energy profiles are for the Southern Bean Mozaic Virus [82] computed for two extreme orientations of the Thr -OH ligands of the selectivity filter: one, when the H ends of the -OH dipoles are rotated so that they face maximally *in* toward the lumen of the channel, the other, when they are rotated so as to face maximally *away* from the lumen. A partial charge of +0.100 has been assigned to the H atom and of −0.100 to the O atom of the -OH group. The top half of the figure plots the profiles calculated for K, the bottom half for Cl^-. The left half of the figure shows the energy profiles when the -OH groups are rotated maximally *inward* toward the channel axis in the positions shown at the bottom right of Fig. 1. The right half of the figure shows the profiles when they are rotated maximally *away* from the axis in the positions shown at the bottom left of Fig. 1

barrier on the inside being somewhat higher than that on the outside. Similar results are found for other cations [29]. One therefore can conclude that this type of channelog can bind cations and that its external portion could be permeable to them, but only under conditions when the -OH groups can face away from the fivefold axis.

Anion Permeation Typified by Cl

In the case of Cl^-, illustrated at the bottom of Fig. 5, the situation is essentially reversed. When the Thr -OH's face *in*, a clear energy minimum corresponding to a favorable binding site is seen (Fig. 5, bottom left). When the Thr -OH's face *away*, the site becomes less distinct, though it is still present. For all orientations of the -OH group the external portion of the channel should therefore be permeable to anions. Similar profiles are seen for the other halide anions, with species differences that will be discussed under "selectivity." The results imply that the ring of side-chain -OH ligands can form a selectivity filter in the 4SBV channelog that can bind Cl and K equally well when the -OH ligands are oriented appropriately. Because the -OH group is free to rotate around the C–OH single bond the -OH ligand is thus capable of being "ambidextrous."

Various Contributions to the Energy Profile

The various energies that go to make up the energy profiles of Fig. 5 are now examined. This is done in Fig. 6, where the main differences between cationic and anionic behavior can be seen to originate in the "ion-charge" (i.e., coulomb) energy, which is attractive (negative) at the selectivity filter for Cl^- (Fig. 6, bottom left) and repulsive for K (Fig. 6, top left) when the positive end of the -OH dipoles are rotated *in*. When the -OH dipoles are rotated *away* from the axis, the reciprocating behavior between for cations *vs.* anions is quite apparent (*compare* Fig. 6, upper right and lower right). It is also apparent from Fig. 6 that for

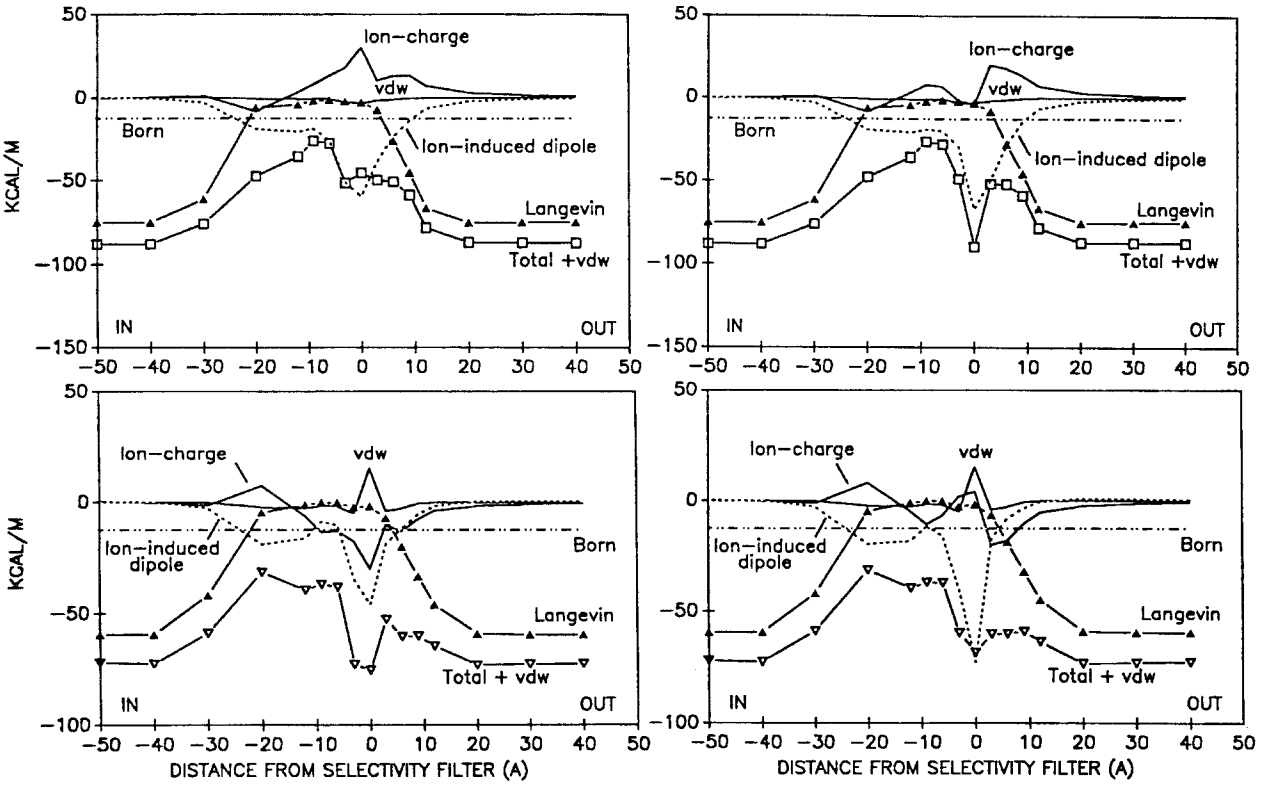

Fig. 6. Energy contributions to the total energy profile for a selectivity filter composed of side-chain hydroxyls. This figure plots the distance dependence of the individual energies that make up the profiles of Fig. 5. The top half of the figure plots the energies computed for K, the bottom half for Cl^-. The left half of the figure shows the energies when the –OH groups are rotated maximally *inward* toward the channel axis. The right half of the figure shows the profiles when the –OH groups are rotated maximally *away* from the axis. Note the reciprocating behavior between anions *vs.* cations in the "ion-charge" (i.e., coulomb) energy. Also note that there are substantial noncoulomb (i.e., "ion-induced dipole") attractions at the selectivity filter for both cations and anions for all orientations of the –OH groups

the frozen coordinate PDLD calculation the "ion-induced dipole" energies make a very important attractive contribution to the energy at the selectivity filter for both cations and anions, particularly when the –OH dipoles face *away*. Indeed, it can be seen in Fig. 6, upper right, that this term is the major component leading to the favorable binding energy for K found in the upper right part of Fig. 5. This "ion-induced dipole" energy also is the source of the persistence of the favorable binding energy for Cl^- when the –OH groups are rotated from their coulombically anion-favoring electrostatic orientation in Fig. 5, lower left, to the coulombically less favoring one in Fig. 5, lower right. In fact, the "ion-induced dipole" energy is so strong in Fig. 6, lower right, that it actually overrides a repulsive coulombic "ion-charge" interaction between Cl^- and the oxygen end of the –OH dipole in this orientation to produce the energy minimum at the selectivity filter mentioned in Fig. 5, lower right.

It should be noted that the PDLD calculations on a frozen structure probably overstate the importance of ion-induced dipole interactions and understate the importance of ion-charge interactions (because the structure has not been allowed to rearrange to optimize ion-charge interactions). Aqvist and Warshel [3] have shown that when a structure has been energy minimized, it rearranges so that ion-charge interactions generally increase at the expense of ion-induced dipole interactions.

Acetylcholine Receptor Channel

We now turn to what can be learned by carrying out PDLD calculations on a conjectured structure for a known channel. We will compute the energy profiles expected for ion permeation down the axis of a frozen pentameric structure proposed for the 23-residue M2 segment of the acetylcholine receptor channel by Oiki et al. [17], using coordinates provided by V. Madison for a minimum energy structure obtained with the CHARMM program for five parallel helices with C5 symmetry and dihedral angles constrained (in the absence of solvent or ions) to regular

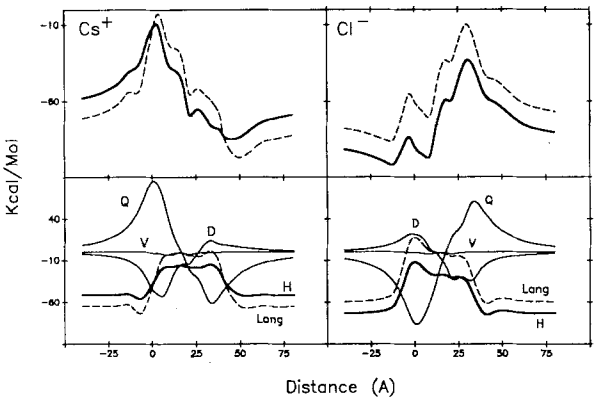

Fig. 7. Energy profiles calculated for Cs^+ and Cl^- permeation through the M2delta pentamer with no excess charges on Glu, Lys, or Arg residues. Inner surface (cytoplasm) is shown to the left, outer to the right. The total energy is plotted in the upper part of the figure, and the separate energy contributions in the lower, labeled as follows: *Q* for ion-charge, *D* for ion-induced dipole, *V* for Van der Waal's, *H* for "refined" hydration, and Lang for "raw" Langevin. Calculations were made using two explicit water molecules (*see* [30] for details). The channel extends from roughly −5 to +40 Å on this figure, with its cytoplasmic end at the left and its extracellular end at the right

helical values. We use Madison's coordinates without further optimization for the presence of water or ions in the channel interior, except that we optimize the orientation of the –OH side chain of the five SER_8 residues in two extreme configurations by allowing the H to rotate maximally toward (for anions) or away (for cations) from the channel axis. The present findings supplement those of an earlier modelling of the AChR channel by Furois-Corbin and Pullman [37–39] who considered a number of alternative structures.

Because the Langevin dipole calculation underestimates hydration in narrow regions of a channel, a refinement in computing the hydration energy has been introduced [30] which involves including a linear hydration of the permeant ion by two explicit water molecules to give a more realistic, "refined" estimate of the energy in the narrowest region of the channel, together with an appropriate scaling of the computed energy when the ion is very distant from the protein so as to match the experimentally known hydration energies in the bulk solution.

"Helix Dipoles" can Cause a Sterically Open Structure to be Impermeable to Ions

The energy profiles computed for cation and anion permeation are shown in Fig. 7. The solid curves in the upper part of the figure show, for Cs^+ and Cl^-, the total energy calculated using the PDLD algorithm with "refined" hydration energy [30]. The dashed curves show the results using the "raw" Langevin procedure without explicit water molecules. The lower part of the figure shows the various energy contributions to these totals. (Incidentally, the dashed and solid curves do not converge at large distances because only the "refined" hydration energy has been scaled to yield the exact value for the experimental free energy of hydration while the "raw" Langevin energy only approximates this.) Considering Cs^+ first, notice that the *N*-shaped total energy profile does not resemble the kind of profile usually associated with an ion-permeable channel [47, 60]. In particular, there is a barrier of at least 50 kcal/M encountered by an ion entering the channel from the cytoplasmic (left) side and an even higher barrier for an ion leaving the channel toward the cytoplasm. This means that the channel, despite being visually quite open, is effectively impermeable to cations. The origin of this barrier is not an artifact of the refined model for hydration, since it is even more pronounced if the calculations are done with the same "raw" Langevin procedure that was used for the virus (dashed curves). The source of this barrier can be seen in the lower part of Fig. 7 to be the repulsive ion-charge interactions, *Q*, which are largely due to the parallel orientation of the five helix backbones. It is a so-called "helix dipole" [48] effect, as was verified by carrying out the same calculations for the pentameric polyglycine analogue [30], which yields profiles quite similar to those of Fig. 7. A similar, but reciprocal, behavior is expected for anions, as shown for Cl^- at the right of Fig. 7. Therefore an invisible, but substantial, electrostatic barrier to ion permeation is present for the structure postulated by Oiki et al. [17]. This calculation shows how parallel alpha helices can produce such a large electrostatic potential on a channel's axis that, if uncompensated, a sterically quite open channel could be completely impermeable to ions! Similar barriers can be anticipated to be present in other postulated parallel aggregates of alpha helices [61].

Ionization of Side Chains can Compensate the Helix Dipole

Though the helix dipole effect may be less severe in the native channel, where opposing dipoles from other antiparallel alpha helixes are present [38, 43], the dipole effects are not likely to be completely neutralized in the channel if M2 lies closest to the channel axis, as is believed [36, 37, 43]. It should therefore be of considerable interest that differential ionization of the rings of carboxyl and amino residues known to be present at the ends of the channel can produce an almost perfect compensation of such a dipole barrier, as will now be demonstrated.

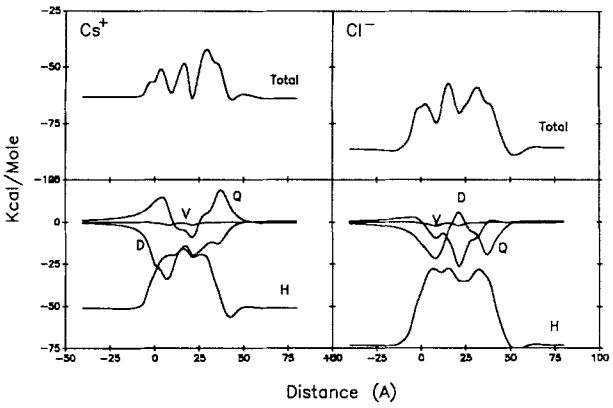

Fig. 8. Energy profiles for Cs^+ and Cl^- permeation through the M2delta pentamer with excess charge of -3 distributed over the five Glu_1 carboxylate O's, an excess charge of $+1$ distributed over the five Lys_2–NH's, and an excess charge of $+2$ distributed over the five Arg_{23} guanidino residues. Calculations were made using two explicit water molecules (*see* [30] for details). The channel extends from roughly -5 to $+40$ Å on this figure, with its cytoplasmic end at the left and its extracellular end at the right

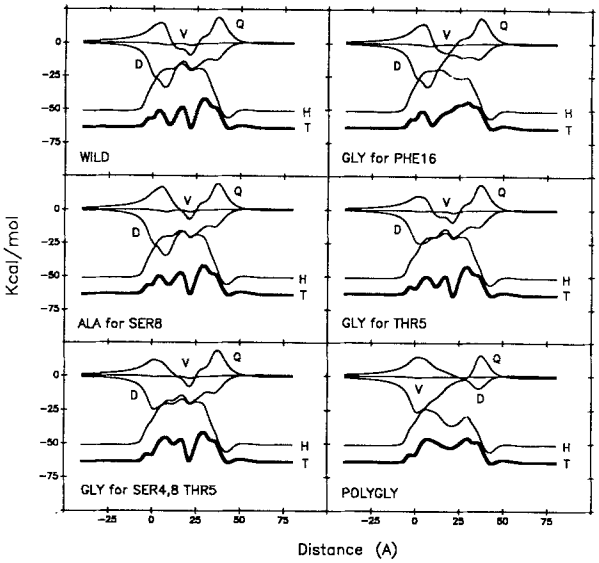

Fig. 9. Energy profiles for Cs^+ permeation through the indicated "computer mutants" of the M2delta pentamer. The channel extends from roughly -5 to $+40$ Å on this figure, with its cytoplasmic end at the left and its extracellular end at the right. The total energy (T) is indicated by the thickest curve. This is described in the text

The existence of rings of ionizable GLU and LYS side chains at the cytoplasmic end of the M2 segment and of ARG side chains at the extracellular end and their importance for conductance has been pointed out [50, 51], and the likely role of these residues in modulating cation *vs.* anion selectivity in ligand-gated channels quite generally is well appreciated [1, 4, 37]. Another property of such groups is their ability to compensate the helix dipole potential by alterations in their state of dissociation, which is regulated by the local H^+ concentration. Since the free H^+ concentration is decreased by a positive dipole potential and increased by a negative one, the inner, cytoplasmic end of the channel will tend to become negatively charged while the outer, extracellular end will tend to become positively charged. These potentials provide a negative feedback compensation of the dipole, which can be almost perfect. This is shown in Fig. 8 where the energies have been computed for Cs^+ (left) and Cl^- (right) for the situation in which three protons have been assumed to be dissociated from the ring of GLU carboxylates, one proton has been bound to the ring of LYS amines, and two protons have been bound to the ring of ARG amines, maintaining a channel which is neutral overall, but negatively charged at the left and positively charged at the right, compensating the helix dipole. This is done by placing an excess charge of -0.3 on each of the 10 delta oxygens of GLU, $+0.1$ on each of the 10 zeta hydrogens of LYS, and $+0.1$ on each of the 20 eta hydrogens of ARG; so that each ring of charge has following excess: GLU (-3), LYS ($+1$), ARG ($+2$).

It can be seen that the dipole term has been almost perfectly compensated, yielding an energy profile that is quite reasonable for Cs^+ permeation. This energy profile shows two clear binding sites and three barriers, with the largest barrier being toward the exterior. The Cl^- energy profile, while no longer showing the dipole barrier, nevertheless represents an anion-impermeant situation in being an elevated plateau with two extremely low affinity anion binding sites. Considering the restriction of "frozen" coordinates in the modelling and the possibility (not yet explored) that the minimum energy path may not lie along the channel axis, the profiles for both Cs^+ and Cl^- are now surprisingly compatible with experimental data, for they imply that the channel should be cation selective and show a rate of cation permeation approaching that observed experimentally [1, 14].

Exploring Structure-Function Relationships by Computer Mutation

It is possible to examine the origins of the local energy minima and maxima that produce the computed energy profile by replacing individual groups by sterically compatible residues, i.e., by "mutating" the channel and recomputing the energy profiles. Figure 9 presents the results for Cs of a series of computer "mutations" on a wild-type channel with the original M2delta residues and with the initial profile of Fig. 8, shown at the top left and labeled

WILD. No energy minimization of the structure was done after the amino acid residue replacement. The channel extends from roughly -5 to $+40$ Å on this figure, with its cytoplasmic end at the left and its extracellular end at the right. The total energy (T) is indicated by the thickest curve.

The lower right of Fig. 9 shows the computed energy profile for a channel (labeled *POLYGLY*) in which all residues except the charged GLU_1, LYS_2, and ARG_{23} residues have been replaced by glycines. This profile is relatively featureless and provides a useful comparison with the wild-type channel and with the other mutations. Notice that the largest barriers to cation permeation correspond to the regions in which the greatest loss of hydration occur. Also notice that the energy level in the channel is elevated over that in solution by only about 13 kcal/M, much less than would occur on taking a Cs^+ ion out of water into a low dielectric medium. This supports the conclusion of Furois-Corbin and Pullman [36–38] that bundles of apolar alpha helices can provide a permeation pathway for ions (*also see* [56]). It is, however, apparent that the nonspecific interactions with the polyglycine backbone are insufficient to make this structure almost as favorable for cation permeation as it is when lined with polar residues (*compare* this with the profile for the wild-type channel).

Replacing SER_8 by ALA (labeled *ALA for SER8* in Fig. 9) substantially decreases the depth of the internal cation binding site located about 10 Å from the inner face. This observation is consistent with the experimental demonstration [63] that such a mutation reduces the residence time of a positively charged inhibitor of ion conductance. In certain concentration ranges, it would also be expected to reduce outward current, as these authors also observe. An equally large contribution to the cation affinity of the internal cation binding site appears to come from the five THR_5 residues that form the narrowest portion of the channel. This is evidenced by the effects of replacing THR_5 by GLY (labeled *GLY for THR5* in Fig. 9). Here the depth of the inner binding site is reduced slightly more than when SER_8 is replaced by ALA (or by GLY, *not shown*). Indeed, Fig. 9 labeled *GLY for SER4,8 THR5* at the lower left shows that it is necessary to replace SER_4 and THR_5 in addition to SER_8 by GLY (or ALA) to remove the inner cation binding site completely.

The origin of an unexpected second, more external, cation binding site not attributable to polar groups is explored in Fig. 9. This energy minimum for this site is apparent at around 22 Å in the wild-type channel but is absent in the GLY for PHE_{16} "mutation" at the top right, indicating that it is the aromatic phenylalanine side chains that provide the favorable interactions for cations at this site. This is surprising if one thinks of ion-charge interactions as the only important ones, and it remains to be seen if this conclusion applies to an energy-minimized structure, or whether it is an "artifact" of the PDLD procedure which can exaggerate the magnitude of ion-induced dipole energies in a nonenergy-minimized structure.

Discussion

These computations on the M2delta pentamer with frozen coordinates have revealed a number of features of interest to ion permeation, but such modelling is too crude to be expected to predict the observed selectivity, a much more stringent criterion. The expected selectivity for such a frozen wide channel is intuitively expected to be lyotropic ($Cs > Rb > K > Na > Li$). But experimental data already suggest that the monovalent and divalent binding sequences are nonlyotropic [1, 14], and T. Konno and B. Sakmann (*personal communication*) have recently demonstrated a conductance selectivity sequence $K > Rb > Cs > Na > Li$ for the wild-type AChR channel expressed in frog oocytes, as well as a sequence $Rb > Cs > K > Na > Li$ for certain mutants. Whether possible structural rearrangements can occur under energy minimization of a water-filled structure to produce the observed selectivity among cations remains to be explored. This brings us naturally to an examination of removing the constraint to frozen coordinates by molecular dynamics simulations.

II. Energy-Minimized PDLD (EM/PDLD) Calculations for the Gramicidin Channel

At the cost of considerably more extensive computations, it is possible to remove the constraint to frozen coordinates by using a molecular dynamics simulation to relax the protein structure and optimize the free energy of the channel for various positions as an ion is moved through it. Aqvist and Warshel have carried out such a study for gramicidin [3], which constitutes an excellent prototype for this procedure.

The channel formed in bilayers by the peptide antibiotic gramicidin is unique in being the only channel for which high quality permeation data exist and in which the structure is well enough defined for theoretical predictions to be directly compared with experimental data. However, despite its known crystal structure in several conformations [91, 59] and well-defined electrical behavior [2, 28], the actual locations of the atoms in the beta helical functional form [87] are still really not known. This is probably because the molecule is so small and flexi-

ble that its conformation can vary with the species of ion within the channel, as well as with its position and occupancy state. In this sense, the channel within the gramicidin dimer may be a more difficult structure to deal with than the channels between protein subunits because these latter structures are stabilized by many internal contacts within, as well as between, subunits.

A large number of theoretical studies have been carried out for the gramicidin channel (*see* [3, 54] for references). These range from continuum electrostatic treatments [53] to microscopic calculations involving energy minimization [32, 74, 85], Monte Carlo [57], and molecular dynamics simulations [62, 65]. However, although these studies provide much valuable information, they are disappointing in the differing, and generally unrealistically large, values they predict for the energy difference between the outside and the central region of the channel. Indeed, prior to the studies by Aqvist and Warshel [3] summarized below, only the treatment by Sung and Jordan [85] appears to have reproduced a reasonable energy profile even though bulk solution effects were not treated. The principle difficulty with all conclusions about energy profiles prior to Sung and Jordan's and Aqvist and Warshel's has been the restriction to frozen coordinates. It is interesting that such a simple model as Sung and Jordan's, which removes this restriction by allowing the individual dipoles of the backbone to reorient, can capture the essence of the profile.

Aqvist and Warshel used an approximate but complete representation of the entire system rather than a rigorous treatment for some parts of the system while neglecting others. They performed calculations on energy-minimized forms of Urry's head-to-head dimer for the beta helical conformation of the gramicidin channel [87] and have compared the results obtained with the EM/PDLD procedure with those obtained using MD/FEP simulations. The Aqvist and Warshel study is a prototype for evaluating the free energies, as well as minimum energy structures, for channels whose atomic coordinates are allowed to rearrange as ions, together with a certain number of explicit water molecules, are moved through them. These authors carried out the PDLD treatment of gramicidin to evaluate a complete electrostatic free energy profile for Na in essentially the same way as has been done in the previous sections for the viral and AchR channels, except that for each position of the ion an energy-minimized (instead of "frozen") structure was used. They then applied the MD/FEP procedure to evaluate the electrostatic free energy of Na^+ in the middle of the channel. In their procedure the Na^+ ion is gradually charged from 0 to +1, while the configuration space is sampled by molecular dynamics simulations. A thermodynamic perturbation method is used to evaluate the corresponding electrostatic free energy. In addition, they computed the hydration energy of Na^+ by free energy perturbation simulations with a surface-constrained, all-atom model [94] including 100 explicit water molecules and incorporating dynamical polarization surface constraints.

Three results of their studies validate the use of the EM/PDLD approach for the calculation of permeation behavior in ionic channels. Since this is computationally much less demanding than the MD/FEP procedure described in the next section, these findings deserve mention. First is the agreement between the results of the PDLD and MD/FEP methods in computing the free energy of the Na^+ in the middle of the channel. Second is the agreement between their calculated activation energy barriers and those observed experimentally [28]. Third is the similarity of their predicted energy profile to that of the most reliable of previously existing treatments of permeation [85].

III. Molecular Dynamics Free Energy Perturbation (MD/FEP) Calculations for the 2STV Channelog

This section describes the procedure and presents preliminary results of ion-water and ion-protein interactions for 2STV calculated using the well-known molecular dynamics and free energy perturbation (MD/FEP) procedure (Zwansig [102], *see,* for example [97]) using the MOLARIS program [93], following Aqvist and Warshell [3]. The MOLARIS code was provided by Arieh Warshel and run on an Ardent Titan minisupercomputer using Amino76.lib parameters.

Computation

The MD/FEP procedure calculates the energy of charging the ion inside the channel by changing the charge in small steps from fully charged to zero while allowing the neighboring atoms to continuously rearrange their positions so as to optimize their energy. The system consists of the ion, the atoms of the protein, and a sphere of explicit water molecules centered at the position of the ion and filling all the space not occupied by the ion or protein atoms. As the ion is charged adiabatically in successive small steps, the protein atoms and the water molecules within the sphere are allowed to move until their energy is optimized. The energies and the coordinates are stored for each step of charging, and the energies are then mapped for the charging and discharging processes to yield the free energy [93, 97].

The starting structure for MD/FEP calculations is a cylinder extracted from the crystallographic coordinates of Jones and Liljas [52] containing all com-

plete residues which had any atom within a 20-Å distance of the fivefold axis. This structure was "annealed" at 5°K to remove possible bad contacts using 1000 steps of molecular dynamics and a step size of 0.001 psec with no constraints on the ion, waters, or protein atoms within 30 Å of the ion. The coordinates generated by this procedure were the starting point for all subsequent runs.

Two kinds of calculations are presented here. In the first, the *energy profile* is calculated for an ion moving along its optimum free energy path in a rearrangeable channel. In these calculations the ion is constrained harmonically to a series of positions along the channel's axis but allowed to move in a plane normal to the axis. In this way it finds a free energy minimum which need not lie on the channel's axis. In the second, the *selectivity* is calculated for ions of differing size and charge constrained to lie in the plane of the carbonyl ligands. For each position of the ion in the first case, and for each species of ion in the second, the energy of the system was calculated for 11 values of the partial ion charge varying from fully charged to zero in ten steps, each decrementing the charge by 10%. The reversibility of this calculation was checked by repeating the procedure so as to recharge the ion from zero to fully charged.

A typical MD/FEP calculation for a given ion position involves 12 molecular dynamics simulations, each of 1500 steps at 298°K with a step size of 0.02 psec. The ion is constrained in a plane at its desired position and all protein atoms and water molecules within 10 Å of it are allowed to move. All protein atoms more distant are quadratically constrained to their annealed positions. Within the 10 Å radius of the probing sphere a weak harmonic constraint of 0.5 kcal/Å^2 is included. This constraint is conservative for the present purpose of assessing the barriers for entering and leaving the site because it will cause their height to be overestimated. **Run 1** is an initialization run of 1500 steps with the full charge and appropriate Lennard-Jones parameters for the ion in question. **Run 2** is a further 1500 steps for the fully charged ion which produces the first set of energies to be used in the free energy mapping and the coordinates to be used for the next run in which the charge is reduced to 90% of the total. **Run 3** is performed at 80% of total charge, **Run 4** at 70%, etc., until **Run 12** which is carried out for zero charge. In control calculations for reversibility, the entire procedure has been repeated for Na in the plane of the filter in the reverse direction, starting with the uncharged ion and recharging it to the fully charged state.

For each point to be presented in Fig. 10, 1500 different sets of coordinates for the ion, water molecules and protein atoms are obtained. The first 50 structures were discarded and a weighted average

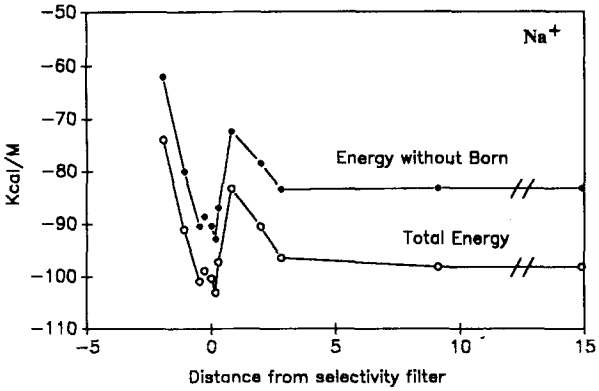

Fig. 10. Optimized free energy profile for Na through the fivefold channelog in the Satelite Tobacco Necrosis Virus calculated by the MD/FEP procedure. The upper curve does not include the Born energy. The lower curve calculates the total free energy including an approximation for the Born energy which varies slightly for different positions in the protein. The extreme right-hand data point is for the hydration of the ion in pure water

energy of the remaining 1450 structures is computed. The energy of charging the ion is calculated from the integration of the energy differences between the successive steps. Thirty-three hours of computer time on an Ardent Titan minisupercomputer were required to obtain the energy for each ion position (about 15 days to construct Fig. 10). The total energy includes the cost of rearranging the water and the protein atoms and all the coulomb interactions of the ions in the system. It leaves out the energy of the interactions of the ion with the induced dipoles in the structure.

Lennard-Jones 6–12 Parameters for Ions in Water

Before carrying out calculations for the protein, it was first necessary to determine a set of Lennard-Jones 6–12 parameters for ions in water which can accurately reproduce simultaneously the experimentally-known free energies of hydration as well as the radial distribution of water molecules. This was done using the MD/FEP procedure on a surface constrained all-atoms solvent model [94] for a sphere of 10 Å radius containing 134 flexible "simple point charge" (SPC) model water molecules consisting of a central oxygen and two hydrogen atoms. This model incorporates angular and radial constraints in order to compensate for the artificial surface created as a result of using a finite number of water molecules. If one assumes the Lennard-Jones parameters for carbonyl oxygens to be the same as for the water oxygens, as we have done here, it is then possible to use these parameters to carry out the same procedure for any location in the protein.

For the Lennard-Jones energy in kcal/M

$$U = A_1A_2/r^{12} - B_1B_2/r^6$$

the following A and B parameters were determined, assuming the same values of 774 (A^{12}[kcal/M]$^{1/2}$) and 24 (A^6[kcal/M]$^{1/2}$) for the oxygen in the water molecule and in a carbonyl group (1 kcal = 4.18 kJ), and starting with the parameters determined previously for Na by Aqvist and Warshel [3]:

	A	B
Li^+	17.3	1.2
Na^+	150	5
K^+	730	14
Rb^+	1206	20
Cs^+	2250	30

Energy Profile and Kinetics for Na

This section is directed to answering the question raised under the PDLD calculations as to whether the barriers for entering and leaving the binding site are so large that it could not exchange ions fast enough to function as a selectivity filter in a channel. Figure 10 presents the energy profile calculated by the MD/FEP procedure for this species. The upper curve plots the free energy profile without the Born contribution. The lower curve includes a crude estimate of the Born energy outside the probing sphere to give the total free energy. Notice in either plot that the barrier for an ion entering or leaving the site from the right (external solution) side has now been reduced substantially (to about 20 kcal/M instead of 60 kcal/M). Such a site would exchange ions with the external solution with a time constant in the order of seconds. An interesting detail is that the site has been "split" into two energy minima on either side of the ring's equator. Extending the calculation to more atoms by increasing the radius to 16 Å of the probing sphere in which explicit water molecules are included and protein atoms are allowed to rearrange further reduces this barrier to about 14 kcal/M. It therefore seems likely that the ring of carbonyl oxygens can actually load and release monovalent ions with sufficient rapidity that such a structure could function as the selectivity filter in an ion-selective channel.

The positions were probed initially in the sequence 0, +1.0, +2.0, +3.0, 0, −1, −2, using coordinates of the preceding position as the starting point for the next one. Intermediate distances were filled in subsequently, and it was verified that the energies were independent of the direction from which they were approached. Several points in the profile were also checked by starting from different initial positions to verify that the profile was independent of the sequence in which the simulations were performed. We will not discuss the barrier toward the inside of the virus here because the height of this is strongly influenced by the (unknown) degree of ionization of the rings of GLU_{140} and LYS_{143} residues 5.5 Å away toward the interior; although it seems likely that even if both rings were fully ionized, H-bonds between them would largely neutralize their local charges.

In Relaxed Structures there are no Large van der Waals Repulsions

It is becoming clear from studying the structural rearrangements and the energy costs associated with them that the present structures relax locally rather easily around a cation, so that van der Waal's repulsion between the ion and its surrounding ligands is not as important in such an energy-minimized structure as it is in a truly rigid one. This is understandable by analogy to the distribution of energy in a system composed of springs of various strengths. The 12th power van der Waal's repulsive interaction corresponds to a very "hard spring"; and the energy of this interaction therefore easily redistributes itself into the "softer springs" of lower power interactions (e.g., coulomb, torsional, H-bond bending, etc.) of surrounding atoms. Thus, relatively minor rearrangements can take place in the atoms immediately adjacent to the ligands of the selectivity filter, and the species-dependent contribution due to van der Waal's repulsions in a rigid filter, described elsewhere [27, 29] and discussed briefly in the next section, is no longer confined to interactions with the nearest-neighbor atoms but becomes distributed over more distant regions of the protein.

Some General Comments on Ionic Selectivity

This paper would be incomplete without some discussion of ionic selectivity, particularly with regard to equilibrium binding. It is possible to use the structurally known annular ion binding sites in the viral channelogs as models with which to assess the properties of a filter that could rearrange itself under the kinds of constraints that actually occur in a protein. This work is in progress, using molecular dynamics procedures to assess the contributions to the energetics of allowing the protein structures to rearrange, and we anticipate that the ultimate description of selectivity in a protein will involve not only the local effects considered in the earliest modelling [15, 16] but also more distant effects, whose importance is already well recognized [75].

It is also possible, at considerably less computa-

tional expense, to apply the PDLD procedure to the structurally known annular ion binding sites in the viral channelogs and use these as model structures on which to deduce the behavior of a *completely rigid* selectivity filter. This has in fact been done elsewhere [27, 29], and some salient findings are summarized below.

Selectivity in Rigid Filters

The selectivity in the easily performed PDLD computation for the *rigid filter* case is of interest in examining selectivity by "sieving," a possibility first proposed by Mullins in 1956 [68, 69]. This situation represents an interesting limiting case for which such a computation actually enables one to assess the *energetics* underlying this seemingly *steric* conception. Two sets of studies have been performed examining this for the backbone carbonyl filters in 2STV and 2RHV [27] and for the side-chain hydroxyl filter in 4SBV [29], with the following main findings. The selectivity was calculated for the ion on the fivefold axis, which is the minimum energy position for a narrow filter. For wider filters where the energy minimum can lie off the fivefold axis we checked that there are only minor differences in expectations [27].

Predicted Selectivity Sequences

We have found using PDLD calculations for filters formed by backbone carbonyl oxygens [27] that a lyotropic binding selectivity sequence Cs > Rb > K > Na > Li is expected for the 4 Å wide aperture of the selectivity filter of the 2RHV virus. In contrast, the Eisenman Coulombic Sequence Va, K > Rb > Na > Li > Cs, is predicted for the 2 Å wide aperture of the selectivity filter of the 2STV virus. The optimum in binding selectivity for K in the narrow filter arises from repulsive van der Waal's energies for the larger ions. The particular shape of the van der Waal's energy curve relative to the shape of the hydration energy curve produces the "molecular asymmetry" [26] underlying the "coulomb topology" [25] which leads to such sequences in a rigid filter. Increasing narrowness of the filter becomes the analogue of increasing field strength in the classical theory.

For the –OH filter in the 4SBV channelog the selectivity filter was calculated by the PDLD procedure [29] to be most selective for Cl^- among the halide anions and most selective for Rb^+ among the alkali cations, independent of the value of partial charge. Eisenman Coulombic Sequences and Topology are predicted for both cations and anions: sequence II (Rb > Cs > K > Na > Li) for cations and AIX (Cl > Br > F > I) for anions (*see* [29, 99] for pattern of anion sequences). These conclusions are independent of the partial charge of the –OH group, but the selectivity between cations and anions does depend on the value of partial charge of the –OH dipole [29]. The larger the partial charge, the more anions are favored over cations, and *vice versa*.

For all structures studied so far only examples of conventional Eisenman selectivity sequences (with minor variants for Li) have been generated. It therefore seems reasonable to infer that such sequences will be the only ones that can be generated by such filters. This implies that a coulomb topology [25] holds for rigid selectivity filters. In such a topology, for reasons given below, filter size becomes analogous to "field strength" (the smaller the diameter of the filter, the higher the apparent "field strength"). Clearly, an Eisenman selectivity sequence is not restricted to systems in which coulomb forces are the primary ones [cf. 35]. What is fundamental to an observed selectivity pattern is the underlying *asymmetry* in the ion-protein *vs.* ion-water interactions which gives rise to the particular differences in ion size dependence of the ion-hydration energies *vs.* the ion-protein energies, as discussed elsewhere [26].

Interestingly, in the calculations for 2STV an aperture the size of a Na ion was needed to produce a selectivity optimum for K, and even an ion as large as Rb was still not severely discriminated against by a 2 Å aperture. However, the van der Waal's radii used for these calculations were parametrized for the Langevin-dipole model of hydration and are somewhat smaller than the van der Waal's radii implied by the more precise Lennard-Jones parameters determined in the MD/FEP calculations presented here for hydration by explicit water molecules. Redoing the PDLD calculations with the more precise radii should not alter the pattern of behavior but should shift the optimum toward smaller ions, so that the optimum will probably occur at the ion size which only slightly exceeds the aperture of the filter.

Relation of the Behavior of Rigid Filters to the Expectations of Classical Selectivity Theory

When the ion-binding site is a frozen ring, all ions of the same charge at the same location have *the same* coulomb and induced dipole interactions with the protein regardless of their size [27]. Thus the only species-dependent contributions to selectivity from interactions with the protein come from van der Waal's interactions with the nearest neighbors, which only become significant when the size of the ion exceeds the size of the filter. (The species-depen-

dent interactions with water, which constitute the other contribution to selectivity, are, of course, independent of the ion-protein interactions. Residual species-dependent effects of hydration of the ion at the selectivity filter are negligible in the Langevin-dipole approximation.)

That the selectivity pattern for ions of the same charge in a selectivity filter with frozen coordinates is totally independent of the partial charge on the ligands of the selectivity filter is initially startling, since the partial charge is a measure of the "field strength" of the ligand, and field strength is the key variable in classical selectivity theory [15–20, 25, *see* 47]. In previous selectivity theory the interaction of an ion with a single site was a strong function of ion size because the ion-site separation was dependent on the ionic size, in contrast to the situation in a frozen structure where this separation is size independent [27]. Even for three-dimensional arrays as modelled by alkali halide crystals [15, 16], cation-anion distances still depend on ionic size, and the crystal lattice energies (Coulomb terms multiplied by a Madelung constant to account for coordination and by a Born exponential repulsion parameter) depend on ion size. Even for more abstract considerations of coordination state to neutral ligands [17, 20], ions were allowed to approach to species-dependent distances from all ligands, and interaction energies consequently continued to depend on ion size. However, note that these treatments (with the exception of the crystals) dealt only with local, nearest-neighbor interactions. Energetic consequences of more distant structural rearrangements were not included.

The fundamental difficulty with PDLD modelling of a frozen structure is that proteins appear to be able to relax quite easily to relieve unfavorable van der Waal's contacts, a conclusion which certainly is borne out so far by our molecular dynamics simulations on the 2STV channelog. It thus seems unlikely that the extreme case of a completely rigid selectivity filter can exist in a protein channel. Despite this, PDLD predictions of selectivity for completely frozen structures may have predictive value if the dissipation of the van der Waal's repulsive energy approximates the way this energy is redistributed in a real, semi-rigid system. If the viral filters are indeed highly stabilized by the many interatomic contacts in the pentameric subunits, the channelogs may represent a physical situation in which selectivity by sieving could actually occur.

Overview

It is now clear that selectivity in a large protein need not be solely a result of local interactions, to which case classical modelling so far has been restricted. More distant interactions are likely to be quite important. A clear example is the demonstration by Quiocho et al. [75] of an anion binding site by suitably oriented helix dipoles in the absence of local polar ligands. An even more extreme example would be allosteric interactions, such as the highly cooperative pairwise binding of Ca ions by physically widely separated Ca-binding loops linked by H-bond networks in Calbindin [46, 90] would be. Selectivity theory, therefore, needs to be extended to take into account such nonlocal effects, which could contribute importantly to the total energy whenever ionic replacements are not strictly isomorphous. For the next stage of understanding selectivity it will clearly become necessary to determine both theoretically and experimentally if a replacement of one ion by another occurs within a strictly rigid structure, produces only a local readjustment of the structure within the first few angstroms, or produces a more global rearrangement of the structure. The free energy cost (or gain) of such rearrangements must be calculated before one can know the structural consequences of substituting one ion for another. Fortunately, laboratory minisupercomputers and existing algorithms now make such calculations feasible.

Only further work to assess the energetic consequences of local and more distant readjustments of protein structure on exchanging ions of differing size and charge will tell what kind of ion radius dependence of cation-site interactions will continue to exist when the ligands of the selectivity filter, and the adjoining regions of the protein, are no longer frozen but are permitted to adjust their coordinates to optimize their energy. But it may be a useful working hypothesis for making selectivity predictions from calculations on rigid structures to regard this redistribution as producing an equivalent effect of ion size by "distributing" the energetic effects of the van der Waal's repulsion over a somewhat wider ensemble of atoms than solely the immediate nearest neighbors. If this hypothesis proves fruitful, it should become possible to predict the ionic selectivity of at least some structures from simple PDLD calculations of their behavior when viewed as rigid systems.

Summary

The above findings can be summarized as follows. Binding affinity selectivity represents a balance between energy of hydration and energy of interaction with the filter, including any conformational energy that occurs if the protein can rearrange. In a *rigid selectivity filter,* where ion-exchange is strictly isomorphous, selectivity is expected to be inversely

related to the hydration free energy (i.e., lyotropic) if the size of the filter exceeds that of the largest ion. Only when the size of an ion exceeds the size of the filter do inversions of selectivity sequence occur in which smaller ions become favored. In this situation it is the van der Waal's repulsion energy that causes the selectivity reversal among ions of the same valence type, and not the partial charge (i.e., "field strength") of the ligands. In a rigid filter field strength is relevant only for selectivity between ions of differing valence and/or sign. On the other hand, in a *deformable selectivity filter,* repulsion energy differences among differing species become negligible, and the major contributions to selectivity come from two factors. One is the "field strength" of the binding ligands, variations in which lead to species differences in electrostatic energies of the ions with the ligands locally. The other is the structural energy change of the protein itself, which is less local and can be quite widespread, even allosteric.

Reliability of Energy Computations

The calculations of the energetics of ion-protein interactions involve several assumptions that should be kept in mind in judging the reliability of the results presented here. Stating these assumptions shows where future research should be aimed for improving such calculations. In this section we summarize our point of view on these assumptions in relation to two key problems which we identify as: (i) how well do we know the structures of the channels? and (ii) how adequate for assessing ion-protein interactions are the current computational chemistry force fields?

Structures

We assume that the crystal structure of the channel-forming protein is a good approximation of the actual structure of the protein in the membrane; but we do not know how different these structures might be. In particular, thermal agitation shakes the molecule so that its structure fluctuates among a variety of possible structures of which the crystal structure represents a time average. The fluctuations are simulated in the molecular dynamics calculations, and such calculations are therefore expected to yield an ensemble of structures that is more realistic than the crystal structure itself. The average structure for such an ensemble might miss the existence of multiple low energy states which are effectively in near-equilibrium with each other (a conceivable example would be the existence of multiple quasi-equivalent binding loci for ion-water ensembles, separated by small energy barriers, which would average out structurally to one apparent ion binding locus or "site"). The portions of the protein that are in contact with water are expected to swell because water molecules could get into the protein structure and the crystal could unpack. Full protein solvation is not included in the calculations presented here. Interaction of the protein with the lipids of the membrane may also make structures other than that of the crystal more probable; such interactions are not included in an explicit way in our calculations.

Models

The model used to describe the ions consists of a point charge and two Lennard-Jones parameters which were calibrated using a flexible SPC water molecule model to give the correct water solvation. We do not yet know how well these Lennard-Jones parameters describe the interactions of the ion with other chemical groups such as the ones that exist at the binding sites of the channels. The *partial charge* of the carbonyl or hydroxyl ligands is an important parameter of classical Eisenman selectivity theory. The partial charges used so far have been calibrated to give good simulations of protein structure and the actions of proteins as enzymes. We have assumed that the partial charges are also correct for ion-protein binding; but this still remains to be tested. Related questions are: how are these partial charges modified by other groups in the protein (e.g., by Taft induction effects)? To what extent are ionizable acidic and basic residues in the site or adjacent to it fully ionized or partially protonated?

How flexible are the protein molecules? Ion binding energies and ion selectivity depend on how deformable is the binding site. The force fields used define how flexible the molecule is and were calibrated to give the correct crystallographic structures. How sure are we that the force field gives the correct flexibility from the ion selectivity point of view?

To answer these questions we are currently checking the energy calculation procedures using the valinomycin-alkali metal ion complexes as a simple test case [22]. So far, we conclude that both the partial charge and the flexibility of the molecule are, of course, very important in defining valinomycin selectivity, but that the default values of force fields and partial charges for MOLARIS used in most of the results presented here can indeed be refined but are quite close to being correct as they are. Aqvist's satisfactory description of the gramicidin energy

profile [3] using this force field and the default parameters is a strong indication that the calculations can be trusted.

This work was supported by U.S. Public Health Services Grant GM 24749, National Science Foundation Grant BNS 84-11033, FONDECYT Grant 1112-1989, and DTI grant B-2805. We thank Chari Smith for her perceptive comments on the manuscript and Arieh Warshel, Johan Aqvist, Fred Lee, Alfredo Villarroel, Francisco Benzanilla, Howard Robinson, and Terry Lydon for their valuable help with theory and methodology.

References

1. Adams, D.J., Dwyer, T.M., Hille, B. 1980. *J. Gen. Physiol.* **75:**493–510
2. Andersen, O.S. 1984. *Annu. Rev.Physiol.* **46,** 531–548.
3. Aqvist, J., Warshel, A. 1989. *Biophys. J.* **56:**171–182
4. Barnard, E.A., Darlison, M.G., Seeburg, P. 1987. *Trends Neurosci.* **10:**502–508
5. Bash, P.A., Singh, U.C., Langridge, R., Kollman, P.A. 1987. *Science* **236:**564–568
6. Bernstein, F.C., Koetzle, T.F., Williams, G.J.B., Meyer, E.F., Brice, M.D., Rodgers, J.R., Kennard, O., Shimanouchi, T., Tasumi, M. 1977. *J. Mol. Biol.* **112:**535–542
7. Boheim, G., Jung, G., Menestrina, G. 1987. *In:* Ion Transport Through Membranes. K. Yagi and B. Pullman, editors. pp. 131–145. Academic, New York
8. Bormann, J., Hamill, O.O., Sakmann, B. 1987. *J. Physiol. (London)* **385:**243–286
9. Brisson, A., Unwin, P.N.T. 1985. *Nature (London)* **315:**474–477
10. Brooks, B.R., Brucoleri, R.E., Olafson, B.D., States, D.J., Swaminathan, S., Karplus, M. 1983. *J. Comp. Chem.* **4:**187–217

10*a*. Burkert, U., Allinger, N. 1984. Molecular Mechanics. ACS Monograph 177. American Chemical Soc. Publ. Washington, D.C.

11. Dani, J.A. 1986. *Biophys. J.* **49:**607–618
12. Dani, J.A. 1989. *J. Neurosci.* **9:**884–892
13. Dani, J.A., Eisenman, G. 1984. *Biophys. J.* **45:**10–12
14. Dani, J.A., Eisenman, G. 1987. *J. Gen. Physiol.* **89:**959–983
15. Eisenman, G. 1961. *In:* Symposium on Membrane Transport and Metabolism. A. Kleinzeller and A. Kotyk, editors. pp. 163–179. Academic, New York
16. Eisenman, G. 1962. *Biophys. J.* **2:**259–323
17. Eisenman, G. 1965. *Proc. XXIIIrd Int. Congr. Physiol. Sci. (Tokyo)* **87:**489–506
18. Eisenman, G. 1969. *In:* Ion-Selective Electrodes. R.A. Durst, editor. National Bureau of Standards Special Publication **314,** pp. 1–56
19. Eisenman, G. 1977. *In:* Ion Selective Electrodes. E. Pungor, editor. pp. 99–148. Akamemiai Kiado, Budapest
20. Eisenman, G. 1983. *In:* Mass Transfer and Kinetics on Ion Exchange. L. Liberti and F.G. Helfferich, editors. pp. 121–155. NATO ASI Series, Martinus Nijhoff, The Hague
21. Eisenman, G., Alvarez, O. 1990. *In:* Ca Transport and Homeostasis. D. Pansu, editor. NATO ASI Series. Vol. H48, pp. 283–289. Springer Verlag, Berlin—New York—Tokyo *(in press)*
22. Eisenman, G., Aqvist, J., Alvarez, O. 1990. *Faraday Symp. Chem. Soc. (in press)*
23. Eisenman, G., Dani, J.A. 1987. *Annu. Rev. Biophys. Biophys. Chem.* **16:**205–226
24. Eisenman, G., Dani, J.A., Sandblom, J. 1985. *In:* Ion Measurements in Physiology and Medicine. M. Kessler, D.K. Harrison, and J. Hoper, editors. pp. 54–66. Springer-Verlag, Berlin—Heidelberg—New York
25. Eisenman, G., Horn, R. 1983. *J. Membrane Biol.* **76:**197–225
26. Eisenman, G., Krasne, S. 1975. *In:* MTP International Review of Science. Biochemistry Series. C.F. Fox, editor. Vol. 2, pp. 27–59. Butterworth, London
27. Eisenman, G., Oberhauser, A., Bezanilla, F. 1988. *In:* Transport Through Membranes: Carriers, Channels and Pumps. A. Pullman, J. Jortner, and B. Pullman, editors. pp. 27–50. Kluwer Academic, Dordrecht—Boston—London
28. Eisenman, G., Sandblom, J.P. 1983. *In:* Physical Chemistry of Transmembrane Ion Motions. G. Spach, editor. pp. 329–347. Elsevier, Amsterdam
29. Eisenman, G., Villarroel, A. 1989. *In:* Monovalent Cations in Biological Systems. C.A. Pasternak, editor. pp. 1–29. CRC, Boca Raton, FL.
30. Eisenman, G., Villarroel, A., Montal, M., Alvarez, O. 1990. *In:* Progress in Cell Research. J.M. Ritchie, P.J. Magestretti, and L. Bolis, editors. Vol. 1, pp. 195–211. Elsevier, Amsterdam—New York—Oxford
31. Ermishkin, L.N., Kasumov, Kh.M., Potseluyev, V.M. 1977. *Biochim. Biophys. Acta* **470:**357–367
32. Etchebest, C., Ranganathan, S., Pullman, A. 1984. *FEBS Lett.* **173:**301–306
33. Finer-Moore, J., Stroud, R.M. 1984. *Proc. Natl. Acad. Sci. USA* **81:**155–159
34. Finkelstein, A., Holz, R. 1973. *In:* Membranes. G. Eisenman, editor. Vol. 2, pp. 377–408. Marcel Dekker, New York
35. Franciolini, F., Nonner, W. 1987. *J. Gen. Physiol.* **90:**453–478
36. Furois-Corbin, S., Pullman, A. 1986. *Biochim. Biophys. Acta* **860:**165–177
37. Furois-Corbin, S., Pullman, A. 1988. *In:* Transport Through Membranes: Carriers, Channels and Pumps. A. Pullman, J. Jortner, and B. Pullman, editors. pp. 337–357. Kluwer, Dordrecht—Boston—London
38. Furois-Corbin, S., Pullman, A. 1989. *Fed. Eur. Biochem. Soc.* **252:**63–68
39. Furois-Corbin, S., Pullman, A. 1989. *Biochim. Biophys. Acta* **984:**339–350
40. Gilson, M.K., Honig, B.H. 1987. *Nature (London)* **330:**84–86
41. Giraudat, J., Dennis, M., Heidmann, T., Chang, J.-Y., Changeux, J.-P. 1986. *Proc. Natl. Acad. Sci. USA* **83:**2719–2723
42. Guy, H.R. 1984. *Biophys. J.* **45:**249–261
43. Guy, H.R., Hucho, F., 1987. *Trends Neurosci.* **10:**318–321
44. Guy, R., Seetharamulu, P. 1986. *Proc. Natl. Acad. Sci. USA* **83:**508–512
45. Harrison, S.C., Olson, A.J., Schutt, C.E., Winkler, F.K., Bricogne, G. 1978. *Nature (London)* **276:**368–373
46. Herzberg, O., James, M.N.G. 1985. *Biochemistry* **24:**5289–5302
47. Hille, B. 1984. *Ionic Channels of Excitable Membranes*. pp. 426. Sinauer, Sunderland, Mass.
48. Hol, W.G.J., van Duijnen, P.T., Berendson, H.J.C. 1978. *Nature (London)* **273:**443–446
49. Hucho, F., Oberthur, W., Lottspeich, F. 1986. *FEBS Lett.* **205:**137–142
50. Imoto, K., Busch, C., Sakmann, B., Mishina, M., Konno, T., Nakai, J., Bujo, H., Mori, Y., Fukuda, K., Numa, S. 1988. *Nature (London)* **335:**645–648

51. Imoto, K., Methfessel, C., Sakmann, B., Mishina, M., Mori, Y., Konno, T., Fukuda, K., Durasaki, M., Bujo, H., Fujita, Y., Numa, S. 1986. *Nature (London)* **324:**670–674
52. Jones, T.A., Liljas, L. 1984. *J. Mol. Biol.* **177:**735–767
53. Jordan, P.C. 1981. *Biophys. Chem.* **B13:**203–212
54. Jordan, P.C. 1987. *J. Phys. Chem.* **91:**6582–6591
55. Jullien, L., Lehn, J.M. 1988. *Tetrahedron Lett.* **29:**3803–3806
56. Karle, I.L., Flippen-Anderson, J., Uma, K., Balaram, P. 1988. *Proc. Natl. Acad. Sci. USA* **85:**299–303
57. Kim, K.S., Clementi, E. 1985. *J. Am. Chem. Soc.* **107:**5504–5513
58. Kosower, E.M. 1984. *Biophys. J.***45:**13–15
59. Langs, D.A. 1988. *Science* **241:**188–191
60. Läuger, P. 1973. *Biochim. Biophys. Acta* **311:**423–441
61. Lear, J.D., Wasserman, Z.R., DeGrado, W.F. 1988. *Science* **240:**1177–1181
62. Lee, W.K., Jordan, P.C. 1984. *Biophys. J.* **46:**805–819
63. Leonard, R.J., Labarca, C.G., Charnet, P., Davidson, N., Lester, H.A. 1988. *Science* **242:**1578–1581
64. Linderstrom-Lang, K. 1924. *Compte. Rend. Trav. Lab. Carlsberg* **15:**1–29
64*a*. Luo, M., Vriend, G., Kamer, G., Minor, I., Arnold, E., Rossmann, M.G., Boeze U., Scraba, D.G., Duke, G.M., Palmenberg, A.C. 1987. *Science* **235:**182–191
65. Mackay, D.H.J., Berens, P.H., Wilson, K.R., Hagler, A.T. 1984. *Biophys. J.* **46:**229–248
66. Mayo, S.L., Olafson, B.D., Goddard, W.A. 1990. *J.Phys. Chem. (in press)*
67. Montelius, I., Liljas, L., Unge, T. 1988. *J. Mol. Biol.* **201:**353–363
68. Mullins, L.J. 1956. *In:* Molecular Structure and Functional Activity of Nerve Cells. R.G. Grennel and L.J. Mullins, editors. pp. 123–166. American Institute of Biological Sciences, Washington
69. Mullins, L.J. 1960. *J. Gen. Physiol.* **43 (Suppl. 1):**105–117
70. Noda, M., Takahashi, H., Tanabe, T., Toyosato, M., Furutani, Y., Hirose, T., Asai, M., Inayama, S., Miyata, T., Numa, S. 1982. *Nature (London)* **299:**793–797
71. Oiki, S., Danho, W., Madison, V., Montal, M. 1988. *Proc.Natl. Acad. Sci. USA* **85:**8703–8707
72. Olson, A. J., Bricogne, G., Harrison, S.C. 1983. *J. Mol. Biol.* **171:**61–93
73. Perutz, M.F. 1989. *Q. Rev. Biophys.* **22:**139–236
74. Pullman, A., Etchebest, C. 1987. *In:* Ion Transport Through Membranes. K. Yagi and B. Pullman, editors. pp. 277–293. Academic, New York
75. Quiocho, F.A., Sack, J.S., Vyas, N.K. 1987. *Nature (London)* **329:**561–564
76. Robinson, H., Crofts, A. 1988. *Biophys. J.* **53:**404*a*
77. Rossmann, M.G., Abad-Zapatero, C., Hermodson, M.A., Erickson, J.W. 1983. *J. Mol. Biol.* **166:**37–83
78. Rossmann, M.G., Abad-Zapatero, C., Murthy, M.R.N., Liljas, L., Jones, T.A., Stranberg, B. 1983. *J. Mol. Biol.* **165:**711–736
79. Rossmann, M.G., Arnold, E., Erickson, J.W., Frankenberger, E.A., Griffith, J.P., Hecht, H.-J., Johnson, J.E., Kamer, G., Luo, M., Mosser, A.G., Rueckert, R.R., Sherry, B., Vriend, G. 1985. *Nature (London)* **317:**145–153
80. Rossmann, M.G., Johnson, J.E. 1989. *Annu. Rev. Virol. (in press)*
81. Russell, S.T., Warshel, A. 1985. *J. Mol. Biol.* **185:**389–404
82. Silva, A.M., Cachau, R.E., Goldstein, D.J. 1098. *Biophys. J.* **52:**595–602
83. Silva, A.M., Rossmann, M.G. 1985. *Acta Crystallogr.* **B41:**147–157
84. Stauffacher, C.V., Usha, R., Harrington, M., Schmidt, T., Hosur, M.V., Johnson, J.E. 1987. *In:* Crystallography in Molecular Biology. D. Moras, J. Drenth, B. Strandberg, D. Suck, and K. Wilson, editors. pp. 293–308. Plenum, New York—London
85. Sung, S.-S., Jordan, P.C. 1987. *Biophys. J.* **51:**661–672
86. Tanford, C., Kirkwood, J.G. 1957. *J. Am. Chem. Soc.* **79:**5333–5339
87. Urry, D.W. 1971. *Proc. Natl. Acad. Sci. USA* **68:**672–676
88. Van Gunsteren, W.F., Berendsen, H.J.C., 1985. *In:* Molecular Dynamics and Protein Structure. J. Hermans, editor. Polycrystal Book Service, Western Springs, IL
89. Van Gunsteren, W.F., Karplus, M. 1980. *J. Comput. Chem.* **1:**260–274
90. Vogel, H.J., Forsen, S. 1987. *In:* Biological Magnetic Resonance. Vol. 7. L.J. Berliner and J. Reuben, editors. Plenum, New York—London
91. Wallace, B.A., Ravikumar, K. 1988. *Science* **241:**182–187
92. Warshel, A. 1979. *J. Phys. Chem.* **83:**1640–1652
93. Warshel, A., Creighton, S. 1989. *In:* Computer Simulation of Biomolecular Systems. W.F. van Gunsteren and P.K. Weiner, editors. pp. 120–137. Escom, Leiden
94. Warshel, A., King, G. 1985. *Chem. Phys. Lett.* **21:**124–129
95. Warshel, A., Levitt, M. 1976. *J. Mol. Biol.* **103:**227–249
96. Warshel, A., Russell, S.T. 1984. *Q. Rev. Biophys.* **17:**283–422
97. Warshel, A., Sussman, F., King, G. 1985. *Biochemistry* **25:**8368–8372
98. Weiner, P.K., Kollman, P.A. 1981. *J. Comput. Chem.* **2:**287–320
99. Wright, E., Diamond, J.M., 1977. *Physiol. Rev.* **57:**109–156
100. Yellen, G. 1987. *Annu. Rev. Biophys. Biophys. Chem.* **16:**227–246
101. Young, E.F., Ralston, E., Blake, J., Ramachandran, J., Hall, Z.W., Stroud, R.M. 1985. *Proc. Natl. Acad. Sci. USA* **82:**626–630
102. Zwansig, R.W. 1954. *J. Chem. Phys.* **22:**1420–1426

Received 17 May 1990; revised 17 August 1990

Appendix

PDLD Procedures for Calculating the Energy Profile

The need for a microscopic treatment compatible with the limited power of a microcomputer led to the development of the protein-dipoles Langevin-dipoles (PDLD) approach by Warshel and his colleagues [81, 92–96], which enables water-containing protein systems to be dealt with microscopically or quasi-microscopically without a huge computational effort. The POLARIS source code containing the PDLD algorithm, as well as the necessary PREPARE program, was obtained from Arieh Warshel and was

rewritten by F. Bezanilla to run on a Definicon DSI/780+ 32-bit coprocessor in an IBM/AT environment. A discussion of the approximations and limitations of the PDLD procedure can be found elsewhere [81, 93, 96]. The PDLD procedure is used to compute two things: the energy profile for ion permeation in a hydrated channel and the binding selectivity for various ions at the selectivity filter.

To calculate ion-charge interactions, Q, and ion-induced dipole interactions, D, the structure is reduced to a set of point charges located at the centers of the atoms. These charges represent the permanent dipoles arising from the unequal sharing of electrons in the covalent bonds. At the center of each atom a polarizability is also assigned. The values of point charges and polarizabilities are assigned using the parameters of Levitt and Lifson [*see* 96]. Since the locations of H atoms are not known from X-ray data, hydrogens are added in standard geometries but, except as specifically noted, without attempting energy minimization for H's that can be rotated around a single bond. H's were not added for side-chain carboxylates since these positions are ambiguous. These groups are, moreover, treated as if uncharged, unless indicated otherwise.

Q, the ion-charge energies are evaluated by summing pairwise the interactions of all the charges of the system and taking the difference between the sum when the probing ion is charged *vs.* uncharged.

D, the charge-induced dipole energy, is the difference between the sum of all the induce-dipole induced-dipole interactions when the probing ion is charged *vs.* uncharged. Since the dipoles screen the electric field, the calculation is done iteratively until constant.

V, the van der Waal's energy, is calculated from a potential energy profile which uses a distance and an energy parameter to define the dynamic dispersion interaction with neighboring atoms. Warshel's and Russell's [96] energy parameters were used with the distance parameter defined in terms of a van der Waal's potential compatible with Pauling ionic radii. The R_p parameters were set to twice the value of the Pauling ionic radii, which gave adequate but not perfect values for hydration free energies using the Langevin-dipole procedure for modelling water (*see* Fig. 6 of [27]).

B, the Born energy is the work of charging a sphere of 12 Å radius from zero to the charge of the ion in a continuum having the dielectric constant 80 of water. (The difference in Born energy when part of this continuum should represent protein is small since the dielectric constant for the protein should be of the order of 10).

Ion-Water and Protein-Water Interactions

Warshel's Langevin dipole procedure was used to evaluate the interactions of the permeant ion with water molecules (and between water molecules and the protein). This approach deals in a realistic, but approximate, way with the extensive, and differing, numbers of water molecules at various points within the channel interior and surmounts the serious convergence problems encountered when representing water molecules microscopically. It replaces a real water molecule by an average effective point dipole located on a grid with a spacing chosen to reproduce the density of water. The average orientation of the water molecules is then represented by a Langevin type function [96, Eq. 53] including a screening function [96, Eq. 13]; and the polarization of the grid of point dipoles is computed iteratively [96, Eq. 52]. The energy is evaluated according to Eq. 32 of [96].

To implement the Langevin dipole procedure, all water molecules are deleted from the crystallographic data and the program is allowed to replace the real water molecules by a grid of average effective Langevin dipoles. The number of Langevin dipoles which the program assigns to replace water molecules turns out to be a convenient way to measure the volume of the channel available to water, correlating nicely with the structure. In the present calculations the grid excludes points within 2.6 Å of the center of all atoms on the protein surface. This may be too severe an exclusion of water molecules in the narrow regions of the channel adjacent to the selectivity filter and may contribute to overestimating the heights of the energy barriers for entering and leaving the filter. In addition, the Langevin dipole procedure was developed to represent an extended three-dimensional array of water molecules and was not designed for use within narrow regions of a channel where such an array is not possible. Aqvist and Warshel have circumvented this problem in modelling the gramicidin channel by including a linear hydration by two explicit water molecules [3].

Ion-Protein Interactions

For the interactions of the permeant ion with the protein, the energies are evaluated by summing pairwise interactions between charges and the permanent and induced dipoles of the protein whose coodinates are known from crystal structure. The ion is represented by a van der Waal's potential energy profile which uses a distance and an energy parameter to define the dynamic dispersion interactions with neighboring atoms. Energies of charge-dipole, charge-induced dipole, as well as dipole-dipole and induced dipole-induced-dipole interactions, are assessed iteratively until constant. Interactions are calculated microscopically for all the atoms previously selected in making the pentamer around the fivefold axis. Further details are given on p. 393 of Russell and Warshel [81].

Equilibrium and Kinetic Selectivity

The equilibrium selectivity is given simply by the difference between the energy of binding and of hydration (i.e., by the difference between the total energy when the probing sphere is at zero distance and when it is at a great distance from the selectivity filter). On the other hand, kinetic selectivity depends on the heights of the energy barriers relative to the hydration or binding energy levels [25, 47].

Theoretical Hydration Energy

The Langevin procedure, assigning Van der Waal's energy parameters to correspond to Pauling crystal radii, is quite satisfactory for Na^+ and Cl^- but less so for larger monovalent cations, overstating their energies for the present parameters. The theoretical values for divalent and trivalent species are also too low [27]. The energy profiles are not seriously affected by these deficiencies since it is more important to choose a continuous Langevin function than to get the hydration energies precisely correct. Including several explicit water molecules reduces these problems substantially [3, 30].